

Novel 2-phenylquinolin-7-yl-derived imidazo[1,5-*a*]pyrazines as potent insulin-like growth factor-I receptor (IGF-IR) inhibitors

Mark J. Mulvihill,* Qun-Sheng Ji, Heather R. Coate, Andrew Cooke, Hanqing Dong, Lixin Feng, Kenneth Foreman, Maryland Rosenfeld-Franklin, Ayako Honda, Gilda Mak, Kristen M. Mulvihill, Anthony I. Nigro, Matthew O'Connor, Caroline Pirrit, Arno G. Steinig, Kam Siu, Kathryn M. Stolz, Yingchuan Sun, Paula A. R. Tavares, Yan Yao and Neil W. Gibson

(OSI) Oncology, OSI Pharmaceuticals, Inc., 41 Pinelawn Road, Melville, NY 11747, USA

Received 1 August 2007; revised 16 October 2007; accepted 17 October 2007

Available online 23 October 2007

Abstract—A series of novel, potent quinolinyl-derived imidazo[1,5-*a*]pyrazine IGF-IR (IGF-IR) inhibitors—most notably, *cis*-3-(3-azetidin-1-ylmethylcyclobutyl)-1-(2-phenylquinolin-7-yl)imidazo[1,5-*a*]pyrazin-8-ylamine (AQIP)—is described. Synthetic details, structure–activity relationships, and in vitro biological activity are reported for the series. Key in vitro and in vivo biological results for AQIP are reported, including: inhibition of ligand-stimulated autophosphorylation of IGF-IR and downstream pathways in 3T3/huIGFIR cells; inhibition of proliferation and induction of DNA fragmentation in human tumor cell lines; a pharmacokinetic profile suitable for once-per-day oral dosing; antitumor activity in a 3T3/huIGFIR xenograft model; and effects on insulin and glucose levels.

© 2007 Elsevier Ltd. All rights reserved.

1. Introduction

The insulin-like growth factor receptor, IGF-IR, is a tetrameric transmembrane tyrosine kinase which, when activated by its cognate ligands insulin-like growth factor-I (IGF-I) and -II (IGF-II), has been implicated as a key driver in certain forms of solid tumors and hematologic neoplasias.^{1–8} The receptor is composed of two subunits: an extracellular α subunit (responsible for ligand binding) and a β subunit (consisting of a transmembrane and cytoplasmic tyrosine kinase domain). Ligand binding activates intrinsic tyrosine kinase activity, resulting in signaling cascades that progress through the IRS-1/PI-3K/AKT/mTOR and Ras/Raf/MEK/ERK pathways.⁹ These downstream pathways ultimately stimulate cellular proliferation, survival, transformation, metastasis, and angiogenesis. Increased expression of the receptor and/or its ligands has been shown in a broad range of solid tumors and hematologic neoplasias.

The link between cancer and IGF signaling is supported by epidemiological studies showing an increased relative risk for the development of colon, prostate, breast, lung, and bladder cancers in individuals with circulating IGF-I levels in the upper tertile of the normal range.^{10–15} In addition, tumor IGF-IR expression correlates with poor prognosis in renal cell carcinoma¹⁶ and increased IGF-II expression has been noted in a variety of human tumors, including colorectal,^{17,18} ovarian,^{19,20} lung,²¹ and liver.²² Recent data from our research efforts, as well as others, clearly indicate that an active IGF-II autocrine loop plays an important role in colon cancer progression.²³ Reduction of IGF-IR activity has been shown to induce apoptosis in tumors but only produce growth arrest in untransformed cells, suggesting a potential basis for tumor selectivity in therapeutic applications.²⁴ Inhibition of IGF-IR by various approaches, including antisense,^{25,26} anti-IGF-IR antibodies,^{27–30} dominant-negative IGF-IR,^{31–33} and small-molecule inhibitors,^{34–36} has been shown to reduce tumor growth in human tumor xenograft models.^{37,38} We report herein a series of novel and potent quinolinyl-derived imidazo[1,5-*a*]pyrazine IGF-IR inhibitors **2**—most notably, *cis*-3-(3-azetidin-1-ylmethylcyclobutyl)-1-(2-phenylquinolin-7-yl)imidazo[1,5-*a*]pyrazin-8-ylamine **2f** (AQIP)—

Keywords: Imidazopyrazines; Insulin-like growth factor-I receptor; IGF-IR; IGF-IR; Tyrosine kinase inhibitor; Tumor growth inhibition; Cancer.

* Corresponding author. Tel.: +1 631 962 0787; fax: +1 631 845 5671; e-mail: mmulvihill@osip.com

which was shown to affect cell proliferation by inhibiting Akt activation and, in turn, inducing apoptosis. Its pharmacokinetic properties translated into robust anti-tumor activity in a 3T3/huIGFIR xenograft model following once-a-day oral dosing.

2. Results and discussion

Identification of initial key pharmacophoric interactions as well as structural observations based upon ligand-based SAR indicate that the 8-amino, the nitrogen and oxygen acceptors at the 7-position of the imidazopyrazine core and off the meta position of the 1-phenyl moiety, respectively, and a single atom spacer from the oxygen acceptor to a phenyl are important for affinity.³⁶ The 8-amino and N7-position comprise a canonical kinase ATP-binding site hinge binding motif, interacting with E1080 and M1082 in a mode paralleling that of the pyridin-2-one in a recently published IGF-IR structure (PDB ID: 2OJ9).^{35b} An X-ray co-crystal structure³⁹ of the insulin receptor (IR) with an earlier 3-benzyloxyphenyl-derived imidazopyrazine series led to efforts focused on replacing the benzyloxyphenyl moiety with a more constrained quinolinyl moiety. This X-ray structure shows that the methylene and ether oxygen are almost completely coplanar with the proximal phenyl ring and that a modest hydrophobic cavity exists below the proximal phenyl and benzylic carbon. The quinolinyl modification was postulated to maintain the key pharmacophores, for example, the proximal and terminal phenyl rings, as well as fill the unoccupied hydrophobic pocket, replace a potentially metabolically unstable benzyloxyphenyl moiety, and ultimately lock the benzyloxyphenyl moiety into the preferred bioactive conformation (Fig. 1).

Initial proof of concept efforts concentrated on synthesizing the direct 2-phenylquinolinyl analog **2a** of compound **1**. The synthesis began with the treatment of commercially available 7-methylquinoline (**3**) with phenyllithium to afford 7-methyl-2-phenyl-1,2-dihydroquino-

line, which upon exposure to air underwent oxidation/aromatization to 7-methyl-2-phenylquinoline (Scheme 1).⁴⁰ While this air oxidation was a convenient and greener method for small, 1-g scale synthesis, it was advantageous to effect the aromatization on a larger, multigram scale by refluxing with sulfur in methanol. Oxidation of the 7-methyl group with selenium dioxide⁴¹ afforded 2-phenylquinoline-7-carbaldehyde (**4a**) in a 42% three-step yield. A directed *ortho*-metalation of 2-chloropyrazine with a preformed solution of LiTMP followed by quenching with aldehyde **4a** afforded alcohol **5a** in 76% yield.⁴² Mitsunobu reaction of alcohol **5a** with triphenylphosphine, phthalimide, and DIAD followed by treatment with hydrazine afforded amine **6a**. While this direct method worked on a smaller, 1-g scale, purification of the amino product from triphenylphosphine oxide and reduced DIAD byproducts generated in the Mitsunobu reaction proved cumbersome on a larger, multigram scale. Optimization of the reaction by converting alcohol **5a** to its respective chloride via treatment with thionyl chloride, followed by reaction with potassium phthalimide, and then subsequent hydrazine-mediated phthalimide deprotection afforded amine **6a** in a 72% three-step yield. Reaction of cyclobutanecarbonyl chloride with amine **6a** in the presence of DIEA and DMAP in methylene chloride afforded amide **7a**, which upon treatment with neat POCl₃⁴³ afforded 8-chloroimidazopyrazine **8a** in 67% yield. In order to reduce the amount of POCl₃ and facilitate the work-up, the reaction was optimized by using acetonitrile as the solvent and only 1.4 equiv of POCl₃ in the presence of a catalytic amount of DMF, improving the yield to 89%. Treatment of 8-chloroimidazopyrazine **8a** with ammonia in isopropanol in a stainless steel Parr apparatus afforded the desired 8-aminoimidazopyrazine product **2a** in 73% yield.

Inhibition of human IGF-IR was determined in 3T3/huIGFIR transfected cells, a mouse 3T3 fibroblast cell line stably overexpressing human full-length IGF-IR. 3T3/huIGFIR cells form tumors in nude mice and, therefore, represent an IGF-IR driven *in vivo* model.

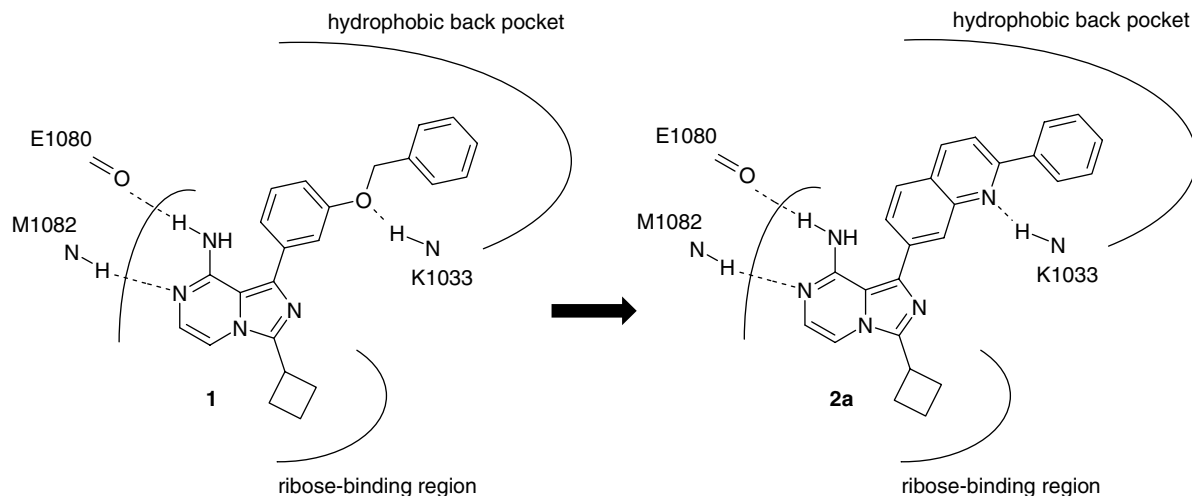
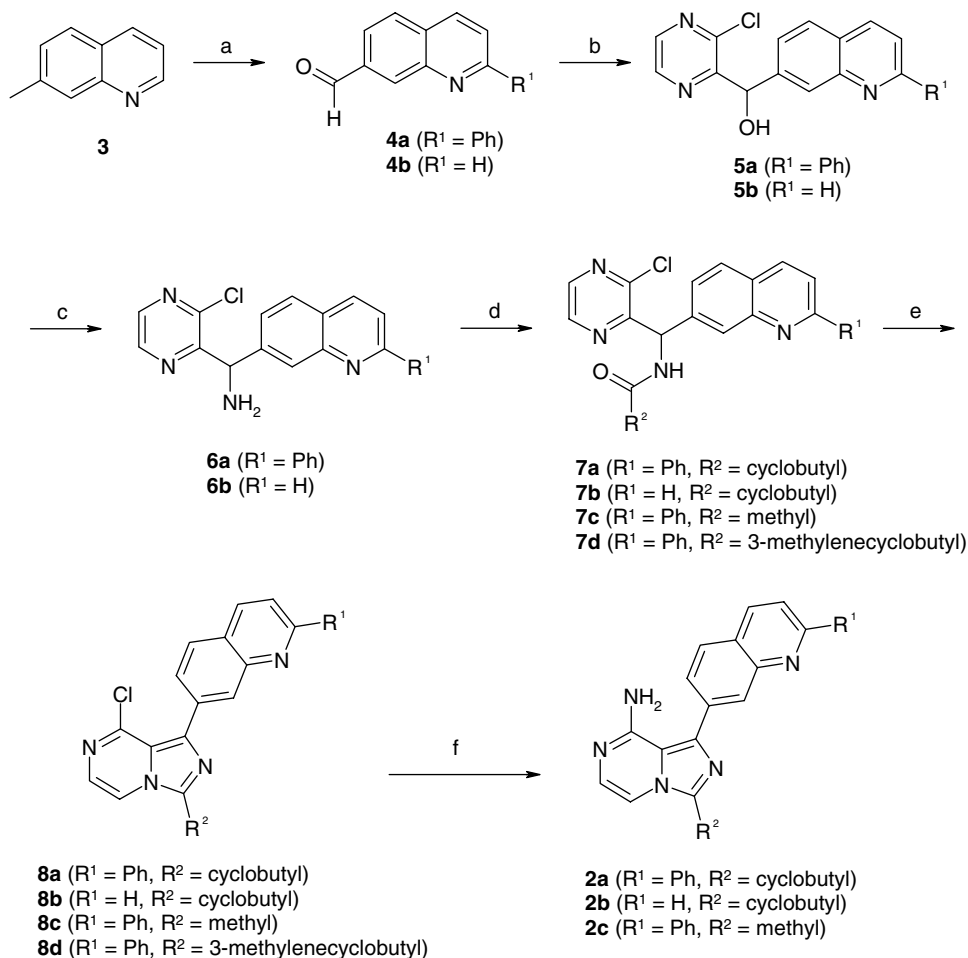


Figure 1. Model of key binding determinants of benzyloxyphenyl-derived imidazopyrazine IGF-IR inhibitor **1** and progression to 2-phenylquinolinyl-derivative **2a**.



Scheme 1. Synthesis of imidazo[1,5-*a*]pyrazine-derived IGF-IR inhibitors **2a–c**. Reagents and conditions: (a) compound **4a**: i—PhLi, THF, 0 °C; ii—sulfur, MeOH, 70 °C; iii—SeO₂, 160 °C (42% three-step yield); (b) *n*-BuLi, tetramethylpiperidine, 2-chloropyrazine, THF, −78 °C; (c) i—SOCl₂, CHCl₃, rt; ii—potassium phthalimide; iii—NH₂NH₂, EtOH, rt; (d) **7a–c**: R²COCl, DIEA, DMAP, CH₂Cl₂; **7d**: 3-methylenecyclobutane carboxylic acid, EDC, HOBT, DIEA, CH₂Cl₂; (e) POCl₃, DMF, CH₃CN, 55 °C; (f) NH₃, *i*-PrOH, 110 °C, 24 h.

The replacement of the 3-benzyloxyphenyl moiety of compound **1** with 2-phenylquinolin-7-yl to afford compound **2a** resulted in a 14-fold increase in cellular potency (Table 1). To confirm the key pharmacophores and to test the binding model, we removed the terminal

Table 1. 3T3/huIGFIR IC₅₀ values for compounds **1**, **2a–c**, and **9**

Compound	X	R ¹	R ²	IGF-IR cell IC ₅₀ (μM)
1	—	—	—	1.16
2a	NH ₂	Ph	Cyclobutyl	0.086
2b	NH ₂	H	Cyclobutyl	>10.0
2c	NH ₂	Ph	Methyl	1.04
9	OH	Ph	Cyclobutyl	>10.0

phenyl ring, replaced the cyclobutyl ring with a smaller methyl group, and also replaced the 8-amino group with a hydroxyl group, synthesizing three key compounds, **2b–c** and **9**, respectively. Based on the binding model, the space occupied by the terminal phenyl cannot be fully occupied by hydrophobic collapse of the nearby residues, suggesting compound **2b** should be inactive. In addition, the hinge interactions are considered critical for affinity. Compound **9** might retain activity, provided tautomerization does not occur. Calculations using the PM3 method in MOPAC suggest the amide tautomer (predicted to be inactive) is favored over the aromatic hydroxide depicted in Table 1. Compounds **2b–c** and **9** were synthesized according to the procedures described in Scheme 1 with two noted deviations. For compound **2c** where R² = Me, acetyl chloride was used in the amide formation step (compound **6a** → **7c**) with the remaining procedures paralleling that for compound **2a**. Compound **9** was synthesized by simply treating compound **8a** with 6 N HCl in THF at 60 °C. It was evident that the terminal phenyl ring as well as the 8-amino group, as exemplified by compounds **2b** and **9**, respectively, were both vital pharmacophores required for IGF-IR inhibition. Truncation of the cyclobutyl moiety to

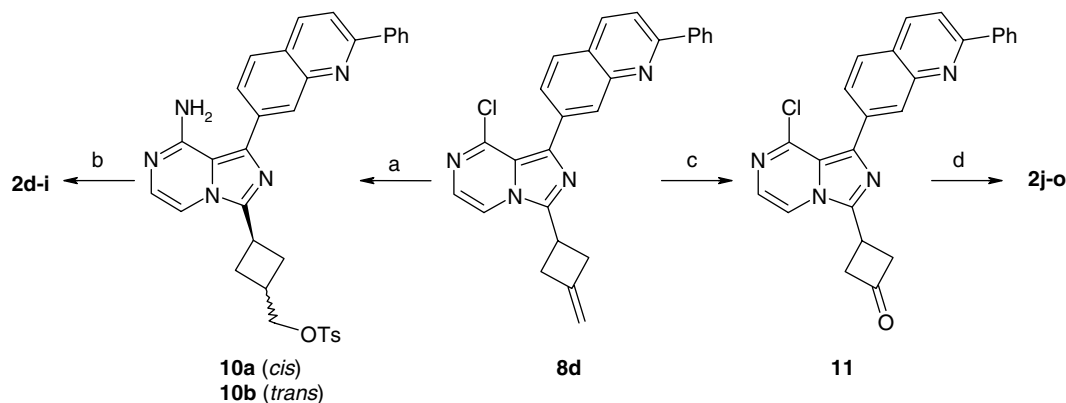
methyl (compound **2a** → **2c**) afforded a 12-fold loss in potency, highlighting that critical mass was required at the C3-position of the imidazopyrazine ring for significant IGF-IR inhibition. These data reinforced previous SAR findings from the benzyloxyphenyl series and indicates that multiple atoms in the ring make non-specific contacts with the protein.³⁶

In an attempt to increase IGF-IR potency and improve solubility, extension of the molecule toward the solvent exposed ribose-binding region of the protein from C3 of the cyclobutyl moiety with substituted-amino and aminomethyl groups was pursued.⁴⁴ Key 3-methylene-cyclobutane intermediate **8d** was targeted, which allowed for the synthesis of both series. Coupling of 3-methylene-cyclobutane carboxylic acid with amine **6a** in the presence of EDC/HOBT afforded amide **7d** in 88% yield, which was subsequently cyclized to imidazopyrazine **8d** in 93% yield with POCl₃ and DMF in acetonitrile (Scheme 1). Hydroboration of 8-chloroimidazopyrazine **8d** with 9-BBN followed by oxidative cleavage afforded a 5:1 ratio of *cis/trans*-hydroxymethylcyclobutyl isomers. When aq NaOH/H₂O₂ was used in the work-up to cleave the carbon–boron bond, the yield was ca. 60% due to the displacement of 8-chloro by hydroxy. A milder reagent, sodium perborate,⁴⁵ was employed and the yield was greatly improved to 95%. This *cis/trans*-mixture was treated with ammonia in a Parr reactor at 110 °C followed by tosylation of the primary alcohol to afford the *cis/trans*-mixture of tosylates, **10a** and **10b**, respectively. At this stage, the isomers were readily separable by silica gel chromatography and both were structurally elucidated by 2D NMR NOE experiments. Displacement of tosylate in compounds **10a** and **10b** with various amines afforded compounds **2d–i**. To further explore tethering out to the solvent exposed ribose-binding region of the protein with a methylene truncated version of aminomethyl derivatives **2d–i**, amino groups were directly linked to C3 of the cyclobutyl ring. Efforts began with the conversion of compound **8d** to cyclobutanone derivative **11** via osmium tetraoxide-mediated dihydroxylation of the exocyclic olefinic moiety followed by sodium periodate oxidative cleavage of the resulting diol. Cyclobutanone **11** was subjected to

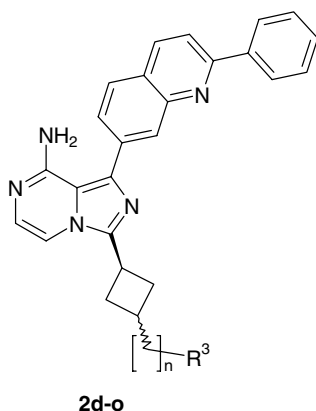
reductive amination with a variety of amines followed by ammonolysis to afford compounds **2j–o**. Interestingly, the reductive amination was highly stereoselective, affording predominately the *cis*-isomer with only a trace of the *trans*-isomer (Scheme 2).

The aminomethylcyclobutyl derivatives **2d–i** were more potent than unsubstituted cyclobutyl **2a** and the *cis*- and *trans*-isomers displayed approximately the same potency, suggesting that both stereoisomers were tolerated and made roughly isoergic interactions with the lip of the ATP-binding pocket and surrounding solvent (Table 2). A clear SAR unfolded around the *cis*-aminocyclobutyl series **2j–o**, where larger cyclic amines such as morpholino (**2o**) were more potent against IGF-IR than dimethylamino (**2j**) or azetidiny (**2k**). In general, the methylene-derived compounds **2d–i** were more potent than the aminocyclobutyl derivatives **2j–n**, and both series displayed an overall improvement in IGF-IR potency and metabolic stability as well as a reduction in CYP3A4 inhibition compared to prototype compound **2a**.

Compound **2f** (AQIP) met the stringent in vitro criteria of CYP3A4 inhibition >20 μM, metabolic stability as measured by predicted extraction ratios (ERs) of <0.60 in both human (hu) and mouse (mu) microsomes, and IGF-IR cellular potency <50 nM, and was progressed to further in vitro and in vivo studies. AQIP, a potent inhibitor of human IGF-IR with a cellular IC₅₀ of 20 nM (Table 3), has favorable microsomal stability across species as represented by the predicted extraction ratios (ERs) of ≤0.70 in human, dog, rat, and mouse, and displays minimal inhibition against a panel of 28 kinases when assayed at ATP concentrations approximating the respective *K_m* value for each form of the enzyme unless otherwise noted (Table 4). The low selectivity between IR and IGF-IR biochemical activity is unsurprising given that the kinase domains of IR and IGF-IR are nearly identical in and around the ATP binding pocket.⁴⁶ When the inhibition of insulin-stimulated p-IR in HepG2 human hepatoma cells was compared with p-IGF-IR inhibition in 3T3/huIGFIR cells, AQIP was approximately 5-fold more selective toward human



Scheme 2. Synthesis of compounds **2d–o** from intermediate **8d**. Reagents and conditions: (a) i—9-BBN, THF, 0 °C → rt (62%); ii—NH₃, *i*-PrOH, 110 °C, 24 h (51%); iii—Ts₂O, pyridine, CH₂Cl₂, −40 °C → rt (53%); (b) Amine, THF, 50 °C; (c) i—NMO, cat. K₂O₈, THF/H₂O, rt; ii—NaIO₄, THF/H₂O (3:1), 0 °C → rt (88% two-step yield); (d) i—Na(OAc)₃BH, THF, amine, DCE, rt; ii—NH₃, *i*-PrOH, 110 °C, 24 h.

Table 2. 3T3/huIGFIR and CYP3A4 IC₅₀ values and microsomal stability for compounds **2a** and **2d–o**

Compound	<i>n</i>	<i>cis/trans</i> -R ³	IGF-IR cell IC ₅₀ (nM)	(ER) microsomal stability mu/hu ^a	CYP3A4 IC ₅₀ (μM)
2a	—	—	86	0.88/0.87	3.4
2d	1	<i>cis</i> -Dimethylamino	19	0.59/0.32	15
2e	1	<i>trans</i> -Dimethylamino	21	0.64/0.75	15
2f	1	<i>cis</i> -Azetidiny	20	0.52/0.28	>20
2g	1	<i>trans</i> -Azetidiny	42	0.71/0.22	17
2h	1	<i>cis</i> -Morpholino	18	0.51/0.61	>20
2i	1	<i>trans</i> -Morpholino	17	0.61/0.76	>20
2j	0	<i>cis</i> -Dimethylamino	148	0.66/0.48	19
2k	0	<i>cis</i> -Azetidiny	147	0.61/0.40	>20
2l	0	<i>cis</i> -Pyrrolidiny	77	0.47/0.55	17
2m	0	<i>cis</i> -Piperidiny	47	0.68/0.55	7.5
2n	0	<i>cis</i> -Thiomorpholino	130	0.88/0.88	7.8
2o	0	<i>cis</i> -Morpholino	18	0.68/0.69	12

^a ER, extraction ratio; mu, murine; hu, human.

Table 3. In vitro profile of AQIP

IGF-IR IC ₅₀ (μM)	Enzyme	0.035 ± 0.002
	Cell (3T3/huIGFIR)	0.020 ± 0.001
IGF-IR vs IR cellular selectivity		5×
CYP3A4 IC ₅₀ (μM)		>20
Microsomal stability (ER)	Human	0.28 ± 0.06
	Mouse	0.52 ± 0.03
	Rat	0.70 ± 0.06
	Dog	0.42 ± 0.03

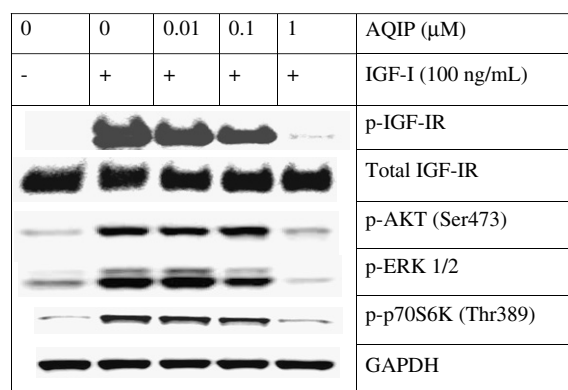
Table 4. Kinase selectivity of AQIP

Kinase	IC ₅₀ (μM)	Kinase	IC ₅₀ (μM)
IGF-IR	0.035 ^a	Rock2	>5
IR	0.076 ^a	RON	5.9 ^a
Abl	>10	SRC	>10
EGFR	9.6 ^a	MEK1	>10
FES	>10	AKT1	>10
FGFR3	>10	PDK1	>30
FYN	>10	PKA	>10
FAK	>10	PKCα	>10
FLT3	>10	P70S6K	>10
KDR	4.3 ^a	Aurora-A	>10
Lck	>10	CDK1/cyclin B	>10
PDGFRβ	>10	CDK2/cyclin A	>10
c-Raf	>10	CDK2/cyclin E	>10
MAPK2	>10	JNK3	>10
IKKβ	>10	CK2	>10

^a Assayed at 100 μM ATP concentration.

IGF-IR than human IR. The increased selectivity in a cellular format suggests that undetermined components, likely exterior to the kinase domains, influence the selectivity ratio of these compounds.

AQIP was tested for inhibition of ligand-stimulated IGF-IR tyrosine kinase activity in intact 3T3/huIGFIR and MCF-7 (data not shown) cells, where it dose-responsively inhibited IGF-I-stimulated phosphorylation of IGF-IR, pAKT, pERK1/2, and p-p70S6K (Fig. 2). Accordingly, in cell-based functional assays, AQIP inhibited IGF-I induced proliferation of 3T3/

**Figure 2.** Inhibition of ligand-stimulated IGF-IR autophosphorylation and downstream pathways in 3T3/huIGFIR cells by AQIP.

huIGFIR cells with an IC_{50} value of 0.05 μ M. The anti-proliferative activity observed in 3T3/huIGFIR cells was extended to a number of tumor cell lines cultured in regular media containing 10% FCS with IC_{50} values ranging from 0.27 to 2.98 μ M. Furthermore, 10 μ M AQIP induced DNA fragmentation in those cells in the presence of 10% FCS (Table 5). Taken together, these data clearly demonstrate that AQIP effectively blocks IGF-IR activation and downstream pAKT and pERK1/2 signaling in tumor cells, which in turn inhibits cellular proliferation and survival.

The pharmacokinetic properties of AQIP were determined following intravenous (iv) and oral gavage (po) administrations in female CD-1 mice, female Sprague Dawley rats, and male Beagle dogs (Table 6). AQIP was dosed at 5, 1, and 2.5 mg/kg iv in saline adjusted to pH 2 with 0.01 mol/L hydrochloric acid and at 25, 50, and 5 mg/kg po in 25 mM tartaric acid in mice, rats, and dogs, respectively (three animals per timepoint). Blood samples were obtained by cardiac puncture from mice and via cannulated veins from rats and dogs, and plasma samples were quantitatively analyzed by HPLC–MS/MS. The PK parameters were calculated by non-compartmental modeling using the median ($n = 3$) concentration at each timepoint for the mouse and concentration–time profiles from individual animals ($n = 3$) for the rat and dog, and are summarized in

Table 5. Inhibition of proliferation and induction of DNA fragmentation in human tumor cell lines by AQIP in normal culture media containing 10% FCS

Cell line	IC_{50} (μ M) for inhibition of cell proliferation	Fold induction of DNA fragmentation over control at 10 μ M
H292	1.95	51 \times
Colo-699	0.69	16 \times
H358	2.98	2.7 \times
HT29	1.26	46 \times
GEO	0.27	4 \times
Colo-205	0.93	0.8 \times

Table 6. Pharmacokinetic properties of AQIP in mouse, rat, and dog

Species	Mouse	Rat	Dog
Route	Intravenous		
Dose (mg/kg)	5	1	2.5
Cl (mL/min/kg)	24	10	30
V_{ss} (L/kg)	10	14	50
$t_{1/2}$ (h)	5.1	19.9	19.0
Route	Oral		
Dose (mg/kg)	25	50	5
C_{max} (μ M)	3.4	1.6	0.17
C_{24h} (μ M)	0.4	0.9	0.09
$AUC_{0-\infty}$ (ng h/mL)	25582	37429	3010
Oral bioavailability (%F)	100	38	94

Note. Cl, clearance; V_{ss} , volume of distribution at steady state; $t_{1/2}$, elimination half-life; C_{max} , maximum measured plasma concentration; C_{24h} , plasma concentration at 24 h; and $AUC_{0-\infty}$, area under the concentration–time curve extrapolated to infinity.

Table 6 (reported values for the rat and dog are means of 3 animals). The oral bioavailability was significantly ($p < 0.05$) lower in rats than in mice or dogs, and although lower bioavailability might be expected from the higher ER in the rat, it is likely that incomplete absorption is a major contributory factor. The volume of distribution increased markedly in the dog compared to the mouse and the rat, and correspondingly the oral exposure is much lower in this species.

The favorable pharmacokinetic profile displayed by AQIP in the mouse, with high oral bioavailability and exposure, led to its evaluation in antitumor efficacy studies. To evaluate antitumor efficacy of AQIP, a 3T3/huIGFIR xenograft mouse model was employed and AQIP was administered orally once daily for 14 consecutive days. In this model, 92% and >100% tumor growth inhibition (TGI) were achieved with 25 and 75 mg/kg of AQIP, respectively ($p \leq 0.001$ for both groups vs control). As is common with molecular targeted agents versus classical cytotoxic agents, antitumor effects at the lower 25 mg/kg daily dose are more cytostatic and, therefore, efficacy is limited to the dosing period; once drug treatment is completed, tumors grow out at similar rates as vehicle treated tumors. Additionally, once tumor volumes reach the predetermined target size of 400%, they continue to grow out at a rate similar to control animals. However, in this model, at the higher dose, we observed approximately 50% maximal tumor regression ($p \leq 0.001$ vs control) during the dosing period and a 15-day growth delay compared to the control group to reach a target tumor volume of 400% (Fig. 3), indicating a dose–response. Overall, at this higher dose, we observed less than a 10% body weight loss (data not shown) during the treatment period suggesting that administration of 75 mg/kg daily is relatively well tolerated.

With the tyrosine kinase domains of the insulin-like growth factor-I and insulin receptors sharing 84% sequence identity,⁴⁶ and only modest (5-fold) in vitro cel-

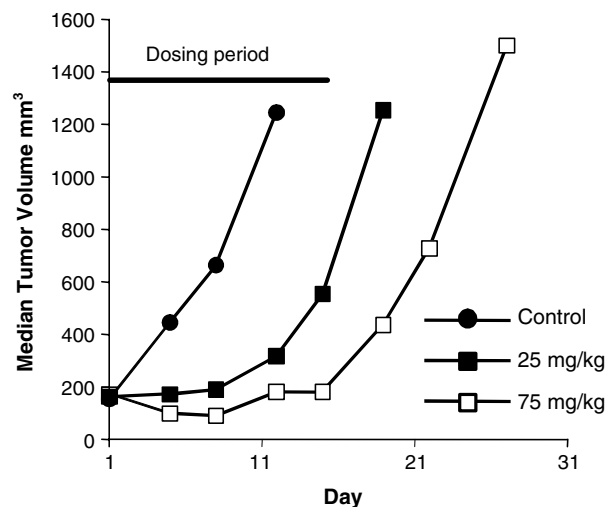


Figure 3. Antitumor activity of AQIP in 3T3/huIGFIR xenograft model.

lular h-IGF-IR versus h-IR selectivity observed with AQIP (Table 3), we were compelled to evaluate the *in vivo* effects of AQIP on insulin receptor inhibition via measuring insulin and glucose levels in mice. The initial study began with measuring blood glucose levels in non-fasted mice following 14 consecutive daily oral doses of 25, 50, or 100 mg/kg of AQIP (Table 7). The 25 and 50 mg/kg doses of AQIP caused little alteration in blood glucose; however, the 100 mg/kg dose caused a significant increase in blood glucose within 4 h of the final dose, with levels remaining elevated in some of the mice for 24–48 h after dosing was discontinued (data not shown). To evaluate the effects of AQIP on glucose clearance, a glucose tolerance test was conducted in mice treated with vehicle alone or with AQIP at oral doses of 25, 50, or 100 mg/kg for three consecutive days (Fig. 4). Upon administration of the glucose load, there was a dose-dependent glucose intolerance in the 50 and 100 mg/kg treated groups compared to the control. At 2 h post-glucose challenge, 44% glucose elevation in mice dosed with the highest dose (100 mg/kg) of AQIP compared to the control animals was observed, whereas the 25 mg/kg dose had no significant effect on glucose clearance. With respect to insulin, mice treated with AQIP for 3 days also had a dose-dependent increase in circulating insulin levels, 4 h post-dosing (Table 8). Taken together, these data indicate that following a 14 consecutive daily oral dosing regimen, 25 mg/kg of AQIP affords significant tumor growth inhibition with minimal effects on blood glucose.

Table 7. Blood glucose in mice following 14 consecutive daily doses of AQIP

Dose (po, qd)	Vehicle	25 mg/kg	50 mg/kg	100 mg/kg
Blood glucose (mg/dL)	138 ± 16	134 ± 29	163 ± 18	242 ± 106
% Change in blood glucose	—	−2.9%	18%	75%

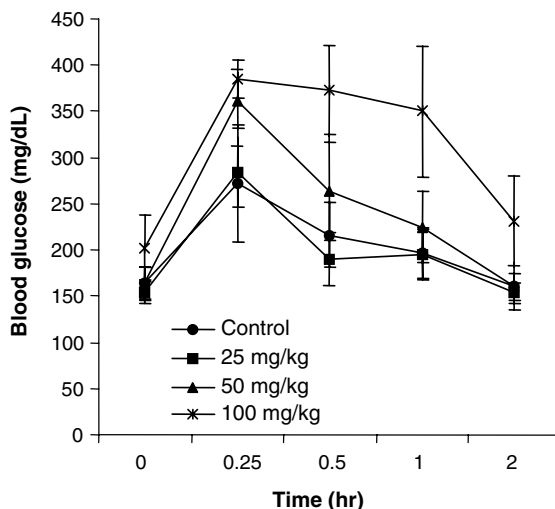


Figure 4. Glucose tolerance test for AQIP in conventional CD-1 mice.

Table 8. Plasma insulin levels 4 h post-final dose with AQIP

Dose (mg/kg)	Insulin levels (ng/mL)
Vehicle control	0.94 ± 0.5
25	13.1 ± 2.8
50	14.7 ± 4.7
100	27.0 ± 2.3

3. Conclusions

In summary, *cis*-3-(3-azetidino-1-ylmethylcyclobutyl)-1-(2-phenylquinolin-7-yl)imidazo[1,5-*a*]pyrazin-8-ylamine (AQIP, compound **2f**) was identified as a novel, highly potent insulin-like growth factor-I receptor inhibitor. AQIP exhibits strong cellular potency against IGF-IR (3T3/huIGFIR cells), modest 5-fold IR selectivity (HepG2 cells), and superior selectivity against a panel of 28 kinases which led to *in vitro* inhibition of proliferation and induction of apoptosis. The pharmacokinetics of AQIP indicated its suitability for once-per-day oral dosing in mouse xenograft efficacy studies, where significant tumor growth inhibition was demonstrated at the 25 mg/kg dose and tumor regression at the 75 mg/kg dose. Despite a dose-dependent elevation in insulin, a minimal effect on blood glucose was observed at the 25 mg/kg dose, suggesting that homeostatic insulin-release mechanisms can compensate for a partial inhibition of IR and maintain glucose uptake *in vivo*. Taken together, these data demonstrate an advance in the field of small-molecule IGF-IR inhibitors, meriting further evaluation of this class of compounds as anticancer agents.

4. Experimental

4.1. General experimental procedures

Unless otherwise noted, all materials/reagents were obtained from commercial suppliers and used without further purification. Reactions were monitored by thin layer chromatography (TLC) on silica gel 60F₂₅₄ (0.2 mm) pre-coated aluminum foil and visualized using UV light. Flash chromatography was performed with silica gel (400–230 mesh). Preparatory TLC was performed on Whatman LK6F Silica Gel 60 Å size 20 × 20 cm plates with a thickness of 1000 μm. Hydromatrix (diatomaceous earth) was purchased from Varian. Mass-directed HPLC purification of compounds was performed on a Waters system composed of the following: 2767 Sample Manager, 2525 Binary Gradient Module, 600 Controller, 2487 Dual λ Absorbance Detector, Micromass ZQ for mass ionization, Phenomenex Luna C18(2) 5 μ 100 Å, 150 × 21.2 mm column with mobile phases of 0.1% Formic Acid Acetonitrile (A) and 0.1% Formic Acid in HPLC water (B). The flow rate is 20 mL/min, run time of 13 min, and a gradient profile of 0.00 min 2% A, 2.10 min 10% A, 8.00 min 50% A, 12.0 min 99% A, 12.8 min 2% A. LC–MS data were collected on either OpenLynx or ZQ3. OpenLynx is an Agilent 1100 HPLC equipped with a Gilson Auto injector and Waters Micromass ZQ for ionization. ZQ3 is an Agilent 1100 HPLC equipped with an HP Series 1100

auto injector and Waters Micromass ZQ for ionization. Both systems use the Xterra MS C18, 5 μ particle size, 4.6 \times 50 mm with a mobile phase of Acetonitrile (A) and 0.01% Formic Acid in HPLC water (B). The flow rate is 1.3 mL/min, run time of 5 min, and a gradient profile of 0.00 min 5% A, 3.00 min 90% A, 3.50 min 90% A, 4.00 min 5% A, 5.00 min 5% A. High resolution mass spectra (HRMS) were obtained by UPLC–TOF–MS on a QStar Pulsar mass spectrometer (Applied Biosystems) using positive turbo ion-spray ionization mode and a scan range of $m/z = 140$ –730 and were accurate to ± 5 ppm. The UPLC system used a Waters BEH C18, 1.7 μ m, 50 \times 2.1 mm column heated to 50 $^{\circ}$ C conditioned with a mobile phase of 10% acetonitrile in 10 mM aq ammonium acetate (A) and acetonitrile (B) and a gradient profile of 0.0 min 0% B, 0.5 min 0% B, 2.3 min 90% B, 2.4 min 90% B, 2.5 min 0% B, 3.0 min 0% B. The flow rate was 0.8 mL/min. Samples were approximately 5 or 10 μ g/mL of each compound in mobile phase A, each also containing an internal standard for mass calibration. ^1H NMR (400 MHz) and ^{13}C NMR (100.6 MHz) spectra were recorded on Bruker or Varian instruments at ambient temperature with TMS or the residual solvent peak as the internal standard. The line positions or multiples are given in ppm (δ) and the coupling constants (J) are given as absolute values in Hertz (Hz). All melting points were determined with a Mel-Temp II apparatus and are uncorrected. Elemental analyses were obtained by Atlantic Microlab, Inc., Norcross, GA.

4.2. Specific procedures

4.2.1. 2-Phenylquinoline-7-carbaldehyde (4a). 7-Methylquinoline (130 g, 0.910 mol) was dissolved in 1 L of dry THF and cooled to below -5°C . Phenyllithium (500 mL, 1.00 mol, 2 M solution in dibutylether) was added dropwise over 30 min while keeping the temperature below 0°C . The mixture was kept at 0°C for 30 min and then allowed to warm to rt for 2.5 h. The mixture was quenched with methanol (200 mL), then water (100 mL) was added, and the organic solvents were removed in vacuo. The product was extracted into EtOAc (3 \times 300 mL), the combined organic layers were washed with brine (200 mL), dried over Na_2SO_4 , and then concentrated in vacuo to yield 207 g (100% yield) of 1,2-dihydro-7-methyl-2-phenylquinoline, which was advanced to the next step without further purification. A mixture of 1,2-dihydro-7-methyl-2-phenylquinoline (201 g, 0.910 mol), sulfur (32.0 g, 1.00 mol), and MeOH (100 mL) was heated at reflux for 16 h. Additional MeOH (1 L) was added to the mixture followed by charcoal (15.0 g). The mixture was heated to reflux and filtered through Celite. The filtrate was concentrated to approximately 400 mL and cooled to 0°C to give a crystalline precipitate which was isolated by filtration (108 g). The filtrate was again concentrated in vacuo and a second crop was isolated by filtration (60.0 g). The solids were combined to afford 168 g of 7-methyl-2-phenylquinoline (84% yield). A mixture of 7-methyl-2-phenylquinoline (50.0 g, 0.230 mol) and SeO_2 (38.0 g, 0.340 mol) was heated to 160°C for 20 h. The melt was cooled to 100°C and DCE (100 mL) was carefully

added to the reaction flask. The suspension was filtered and the filtrate was concentrated in vacuo to a dark brown solid. The compound was purified by silica gel chromatography eluting with 20% EtOAc/Hexanes to afford 26.6 g of 2-phenylquinoline-7-carbaldehyde (50% yield). Mp 112.5 – 114°C . ^1H NMR (CDCl_3) δ 7.48–7.58 (m, 3H), 7.91 (d, 1H, $J = 8.8$ Hz), 7.99–8.02 (m, 2H), 8.18–8.20 (m, 2H), 8.26 (d, 1H, $J = 8.8$ Hz), 8.62 (s, 1H), 10.25 (s, 1H). ^{13}C NMR (CDCl_3) δ 120.9, 122.6, 127.3 (2C), 128.4, 128.8 (2C), 129.7, 130.5, 135.5, 136.4, 137.0, 138.5, 147.6, 158.1, 191.9. MS (ES+): m/z 234.12 (100) [MH^+]. HPLC: $t_{\text{R}} = 3.6$ min (OpenLynx, polar_5 min). Elemental Analysis calcd for $\text{C}_{16}\text{H}_{11}\text{NO}$: C, 82.38; H, 4.75; N, 6.00. Found: C, 82.03; H, 4.59; N, 5.95.

4.2.2. (3-Chloropyrazin-2-yl)-(2-phenylquinolin-7-yl)methanol (5a). A solution of 2,2,6,6-tetramethylpiperidine (0.820 mL, 4.86 mmol) in dry THF (15 mL) at -78°C was charged with n -BuLi (2.5 M in hexanes; 1.95 mL, 4.88 mmol). The reaction mixture was warmed to 0°C for 15 min and then recooled to -78°C . After 5 min, a solution of 2-chloropyrazine (0.370 mL, 4.14 mmol) in THF (0.5 mL) was added. After 25 min, a solution of 2-phenylquinoline-7-carbaldehyde (890 mg, 3.82 mmol) in dry THF (7 mL) was added over a period of 5 min. The mixture was stirred at -78°C for 2 h, warmed to 0°C for 30 min, and then quenched by the addition of citric acid (0.25 M aqueous solution, 15 mL). The mixture was extracted with EtOAc (4 \times 30 mL) and the combined organic extracts were washed with water, NaHCO_3 , brine, dried over MgSO_4 , filtered, and concentrated in vacuo. The crude material was purified by silica gel chromatography eluting with CH_2Cl_2 to 10% EtOAc in CH_2Cl_2 to obtain the desired compound as an off-white foam (1.01 g, 76% yield). Mp 142 – 143°C . ^1H NMR (CDCl_3) δ 4.81 (d, 1H, $J = 8.0$ Hz), 6.25 (d, 1H, $J = 8.0$ Hz), 7.44–7.48 (m, 1H), 7.52 (dddd, 2H, $J = 6.8, 6.8, 0.4, 0.4$ Hz), 7.58 (dd, 1H, $J = 8.4, 2.0$ Hz), 7.82 (d, 1H, $J = 8.0$ Hz), 7.87 (d, 1H, $J = 8.4$ Hz), 8.07 (br s, 1H), 8.12 (ddd, 2H, $J = 7.2, 0.8, 0.8$ Hz), 8.20 (d, 1H, $J = 8.8$ Hz), 8.41 (d, 1H, $J = 2.4$ Hz), 8.62 (d, 1H, $J = 2.4$ Hz). ^{13}C NMR (CDCl_3) δ 72.1, 119.5, 125.7, 126.8, 127.6 (2C), 128.0, 128.3, 128.8 (2C), 129.4, 136.6, 139.4, 141.3, 141.9, 143.3, 147.8, 148.0, 154.2, 157.9. MS (ES+): m/z 347.88/349.90 (3/1) (100) [MH^+]. HPLC: $t_{\text{R}} = 3.3$ min (OpenLynx, polar_5 min). Elemental Analysis calcd for $\text{C}_{20}\text{H}_{14}\text{ClN}_3\text{O}$: C, 69.07; H, 4.06; N, 12.08; Cl, 10.19. Found: C, 69.03; H, 4.03; N, 12.21; Cl, 10.13.

4.2.3. (3-Chloropyrazin-2-yl)-quinolin-7-yl-methanol (5b). A solution of 2,2,6,6-tetramethylpiperidine (0.64 mL, 0.54 g, 3.8 mmol) in dry THF (10 mL), cooled to -78°C , was charged with n -BuLi (2.5 M in hexanes; 1.6 mL, 4.0 mmol). The solution was warmed from -78°C with an ice/water bath for 15 min, followed by re-cooling to -78°C with a dry ice/acetone bath for 10 min, then charged with 2-chloropyrazine (0.29 mL, 0.37 g, 3.2 mmol). After stirring for 30 min, the reaction mixture was charged by cannula with a solution of quinoline-7-carbaldehyde (500 mg, 3.18 mmol) in dry THF (5 mL), cooled to -78°C , and stirred at -78°C for

2.5 h and at 0 °C for 0.5 h. The reaction was quenched by adding 2 mL aq HCl (2 M solution) followed by aq NH₄Cl solution. The mixture was extracted with EtOAc (4 × 30 mL) and the combined organic extracts were washed with water and brine, dried over MgSO₄, filtered, and concentrated in vacuo. The crude material was chromatographed on silica gel [Jones Flashmaster, 20 g/70 mL cartridge], eluting with hexanes/EtOAc 2:1 → 1:1 → 1:4 → EtOAc, yielding the title compound as an orange foam (600 mg, 69% yield). ¹H NMR (CDCl₃) δ 4.87 (d, *J* = 7.6 Hz, 1H), 6.26 (d, *J* = 7.6 Hz, 1H), 7.41 (dd, *J* = 8.4, 4.4 Hz, 1H), 7.60 (dd, *J* = 8.4, 1.6 Hz, 1H), 7.82 (d, *J* = 8.4 Hz, 1H), 8.02 (d, *J* = 0.8 Hz, 1H), 8.14 (dd, *J* = 8.4, 0.8 Hz, 1H), 8.41 (d, *J* = 2.4 Hz, 1H), 8.60 (d, *J* = 2.4 Hz, 1H), 8.91 (dd, *J* = 4.4, 1.6 Hz, 1H). MS (ES⁺): *m/z* 272.1/274.1 (100/38) [MH⁺]. Purity: 94% [HPLC (OpenLynx) at 254 nm].

4.2.4. (3-Chloropyrazin-2-yl)(2-phenylquinolin-7-yl)methylamine (6a). A CHCl₃ (1.63 L) solution of (3-chloropyrazin-2-yl)-(2-phenylquinolin-7-yl)methanol (170 g, 0.490 mol), cooled to -4 °C under N₂ atmosphere, was charged with thionyl chloride (42.7 mL, 0.590 mol) over 10 min. The reaction mixture was allowed to warm to rt and stirred for 4 h. The crude reaction mixture was concentrated in vacuo, dissolved in CHCl₃ and toluene, re-concentrated in vacuo, and then advanced to the next step. 7-[Chloro-(3-chloropyrazin-2-yl)methyl]-2-phenylquinoline (170 g, 0.460 mol) and potassium phthalimide (421 g, 2.27 mol) were dissolved in anhydrous DMF (1.5 L) and heated to 60 °C. After 16 h, the reaction was concentrated in vacuo to a solid, which was suspended in water and then filtered. The solid was washed with water and then re-dissolved in EtOAc and a minimum amount of CH₂Cl₂, which was subsequently washed with water and filtered through a pad of Celite and Na₂SO₄. The resulting filtrate was concentrated in vacuo to afford the desired product as a tan solid (280 g of a 3:1 mix of product/phthalimide, 97% yield), which was advanced to the next step. 2-[(3-Chloropyrazin-2-yl)-(2-phenylquinolin-7-yl)methyl]isoindole-1,3-dione (~3:1 mix with phthalimide, 200 g, 0.42 mol) was suspended in anhydrous EtOH (2.1 L) and CH₂Cl₂ (300 mL), placed under an atmosphere of N₂, and charged with anhydrous hydrazine (105 mL, 3.36 mol). After stirring for 16 h, the reaction mixture was filtered and the solid was washed with EtOH. The filtrate was concentrated in vacuo to a foam, which was purified using silica gel chromatography (EtOAc → 1% 7 N NH₃ in MeOH in EtOAc) to provide the desired compound as a tan solid (82.9 g, 72% three-step yield). Mp 119–120 °C. ¹H NMR (CDCl₃) δ 2.20 (br s, 2H), 5.80 (s, 1H), 7.46 (dddd, 1H, *J* = 6.4, 6.4, 1.6, 1.6 Hz), 7.53 (dddd, 2H, *J* = 8.4, 8.4, 1.2, 1.2 Hz), 7.61 (dd, 1H, *J* = 8.4, 1.6 Hz), 7.81 (d, 1H, *J* = 8.4 Hz), 7.86 (d, 1H, *J* = 8.0 Hz), 8.07 (br s, 1H), 8.13 (ddd, 2H, *J* = 7.6, 2.0, 2.0 Hz), 8.20 (d, 1H, *J* = 8.8 Hz), 8.32 (d, 1H, *J* = 2.8 Hz), 8.60 (d, 1H, *J* = 2.4 Hz). ¹³C NMR (CDCl₃) δ 56.9, 119.1, 125.7, 126.3, 127.4 (2C), 127.6, 128.0, 128.7 (2C), 129.3, 136.4, 139.4, 142.1, 142.3, 144.2, 148.0, 148.1, 156.0, 157.7. MS (ES⁺): *m/z* 346.94/348.89 (3/1) [MH⁺]. HPLC: *t*_R = 2.2 min (OpenLynx, polar_5 min). Elemental Analysis calcd for C₂₀H₁₅ClN₄:

C, 69.26; H, 4.36; N, 16.15; Cl, 10.22. Found: C, 69.15; H, 4.38; N, 16.42; Cl, 10.13.

4.2.5. C-(3-Chloropyrazin-2-yl)-C-quinolin-7-yl-methylamine (6b). A suspension of (3-chloropyrazin-2-yl)-quinolin-7-ylmethanol (600 mg, 2.21 mmol), phthalimide (356 mg, 2.42 mmol), and PS-PPh₃ (loading 2.12 mmol/g; 1.56 g, 3.31 mmol) in dry THF (20 mL), cooled to 0 °C, was charged with DIAD (480 μL, 493 mg, 2.44 mmol). The ice bath was removed and the flask was vortexed at ambient temperature for 21.5 h. Additional PS-PPh₃ (520 mg, 1.10 mmol) and DIAD (160 μL, 164 mg, 0.810 mmol) were added, and vortexing was continued for 6.5 h. The resin was removed by filtration, washed with THF and CH₂Cl₂, and the combined organics were concentrated in vacuo. The crude material was chromatographed on silica gel [Jones Flashmaster, 20 g/70 mL cartridge], eluting with hexanes/EtOAc 3:1 → 2:1 → 1:1 → 1:2, yielding 2-[(3-chloropyrazin-2-yl)-quinolin-7-ylmethyl]-isoindole-1,3-dione as a pale yellow solid (89% yield) which was taken on directly to the next step. ¹H NMR (CDCl₃) δ 7.12 (s, 1H), 7.41 (dd, *J* = 8.0, 4.4 Hz, 1H), 7.54 (dd, *J* = 8.4, 2.0 Hz, 1H), 7.72–7.78 (m, 2H), 7.81–7.89 (m, 3H), 8.01 (d, *J* = 0.8 Hz, 1H), 8.16 (dd, *J* = 8.4, 0.8 Hz, 1H), 8.39 (d, *J* = 2.4 Hz, 1H), 8.50 (d, *J* = 2.4 Hz, 1H), 8.90 (dd, *J* = 4.2, 1.6 Hz, 1H). MS (ES⁺): *m/z* 401.0/402.9 (100/38) [MH⁺]. A solution of 2-[(3-chloropyrazin-2-yl)-quinolin-7-ylmethyl]-isoindole-1,3-dione (789 mg, 1.97 mmol) and anhydrous hydrazine (63.0 μL, 2.00 mmol) in EtOH (4 mL)/CH₂Cl₂ (2 mL) was stirred at rt for 1 d. Additional hydrazine (93.0 μL, 3.00 mmol) was added, and stirring was continued for an additional 2 d. The solid was filtered, washed with EtOH, and the combined organics were concentrated in vacuo to yield a red, sticky solid. This solid was suspended in CH₂Cl₂ and filtered; the filtrate was concentrated in vacuo to afford the title compound as an orange gum (608 mg, 100% yield). ¹H NMR (CDCl₃) δ 2.40 (br s, 2H), 5.79 (s, 1H), 7.39 (dd, *J* = 8.2, 4.2 Hz, 1H), 7.64 (dd, *J* = 8.6, 1.8 Hz, 1H), 7.81 (d, *J* = 8.4 Hz, 1H), 8.01 (d, *J* = 0.8 Hz, 1H), 8.13 (dd, *J* = 8.0, 0.8 Hz, 1H), 8.31 (d, *J* = 2.4 Hz, 1H), 8.59 (d, *J* = 2.4 Hz, 1H), 8.90 (dd, *J* = 4.4, 1.6 Hz, 1H). MS (ES⁺): *m/z* 271.0/273.0 (30/10) [MH⁺], 254.1/256.1 (30/10) [MH⁺-NH₃]. Purity: 97% [HPLC (OpenLynx) at 254 nm].

General procedure A: synthesis of amides 7a–7c. A solution of NEt(*i*Pr)₂ (150 μL, 0.861 mmol), DMAP (5.00 mg, 0.040 mmol), and amine **6** (0.583 mmol) in dry CH₂Cl₂ (5 mL), cooled to 0 °C, was charged with the appropriate acid chloride (0.660 mmol). The bath was removed and the reaction mixture was stirred at rt for 3 h. Water (10 mL) was added, the layers were separated, and the aqueous layer was extracted with CH₂Cl₂ (3 × 15 mL). The combined CH₂Cl₂ layers were washed with water, satd NaHCO₃ solution, and brine, dried over Na₂SO₄, filtered, and concentrated in vacuo to afford the desired amides.

4.2.6. Cyclobutanecarboxylic acid [(3-chloropyrazin-2-yl)-(2-phenylquinolin-7-yl)-methyl]-amide (7a). The title compound was carried forward without further purification as a yellow solid (100% yield). A purified sample

was obtained by crystallization from EtOAc/hexanes to give a light beige solid. Mp 171–172 °C. ¹H NMR (CDCl₃) δ 1.81–1.90 (m, 1H), 1.90–2.02 (m, 1H), 2.11–2.23 (m, 2H), 2.23–2.35 (m, 2H), 3.12 (quint, *J* = 8.4 Hz, 1H), 6.80 (d, *J* = 8.0 Hz, 1H), 7.22 (d, *J* = 8.0 Hz, 1H), 7.43–7.48 (m, 1H), 7.48–7.54 (m, 2H), 7.73 (dd, *J* = 8.4, 2.0 Hz, 1H), 7.82 (d, *J* = 8.0 Hz, 1H), 7.85 (d, *J* = 8.8 Hz, 1H), 7.90 (d, *J* = 0.8 Hz, 1H), 8.07–8.12 (m, 2H), 8.19 (d, *J* = 8.4 Hz, 1H), 8.38 (d, *J* = 2.4 Hz, 1H), 8.58 (d, *J* = 2.4 Hz, 1H). ¹³C NMR (CDCl₃, DEPT135) δ 18.14 (–), 25.18 and 25.30 (rotamers, 2C, –), 39.80 (+), 53.78 (+), 119.42 (+), 126.66 (C_{quart}), 127.12 (+), 127.51 (2C, +), 128.04 (+), 128.16 (+), 128.84 (2C, +), 129.40 (+), 136.53 (+), 139.44 (C_{quart}), 140.81 (C_{quart}), 141.77 (+), 142.99 (+), 148.09 (C_{quart}), 148.34 (C_{quart}), 152.93 (C_{quart}), 157.88 (C_{quart}), 174.02 (C_{quart}). MS (ES+): *m/z* 429.0/431.0 (38/13) [MH⁺], 469.8/471.8 (6/2) [MH⁺ + MeCN]. HPLC: *t*_R = 3.6 min (ZQ3, polar_5 min). Elemental Analysis calcd for C₂₅H₂₁ClN₄O·1/8EtOAc: C, 69.62; H, 5.04; N, 12.74; Cl, 8.06. Found: C, 69.58; H, 5.01; N, 12.69; Cl, 8.15.

4.2.7. Cyclobutanecarboxylic acid [(3-chloropyrazin-2-yl)-quinolin-7-yl-methyl]-amide (7b). The crude material was chromatographed on silica gel [Jones Flashmaster, 20 g/70 mL cartridge], eluting with hexanes/EtOAc 1:1 → 1:3 → EtOAc, yielding the title compound as an orange foam (81% yield). ¹H NMR (CDCl₃) δ 1.81–1.91 (m, 1H), 1.91–2.03 (m, 1H), 2.11–2.23 (m, 2H), 2.23–2.35 (m, 2H), 3.12 (quint, 1H, *J* = 8.6 Hz), 6.80 (d, 1H, *J* = 8.0 Hz), 7.22 (d, 1H, *J* = 8.0 Hz), 7.39 (dd, 1H, *J* = 8.0, 4.0 Hz), 7.77 (d, 1H, *J* = 8.6 Hz), 7.82 (d, 1H, *J* = 8.6 Hz), 7.83 (s, 1H), 8.13 (d, 1H, *J* = 8.4 Hz), 8.37 (d, 1H, *J* = 2.2 Hz), 8.56 (d, 1H, *J* = 2.2 Hz), 8.87 (dd, 1H, *J* = 4.0, 1.6 Hz). MS (ES+): *m/z* 353.1/355.0 (100/39) [MH⁺].

4.2.8. N-[(3-Chloropyrazin-2-yl)-(2-phenylquinolin-7-yl)-methyl]-acetamide (7c). The crude product was chromatographed on silica gel [Jones Flashmaster, 10 g cartridge, eluting with 2% MeOH/CH₂Cl₂] to yield a dark oil (98% yield). ¹H NMR (CDCl₃) δ 2.08 (s, 3H), 6.80 (d, 1H, *J* = 7.9 Hz), 7.26–7.23 (m, 4H), 7.70–7.92 (m, 4H), 8.09–8.11 (m, 2H), 8.17 (d, 1H, *J* = 8.6 Hz), 8.37 (d, 1H, *J* = 2.4 Hz), 8.57 (d, 1H, *J* = 2.5 Hz). MS (ES+): *m/z* 430.84/432.83 [MH⁺].

4.2.9. N-[(3-Chloropyrazin-2-yl)(2-phenylquinolin-7-yl)-methyl]-3-methylenecyclobutanecarboxamide (7d). A CH₂Cl₂ (220 mL) solution of (3-chloropyrazin-2-yl)(2-phenylquinolin-7-yl)methylamine (30.1 g, 87.1 mmol) was charged with EDC (25.0 g, 131 mmol), HOBT (11.8 g, 87.1 mmol), DIPEA (23.0 mL, 130 mmol), and 3-methylenecyclobutanecarboxylic acid (12.7 g, 113 mmol, synthesized according to the procedures described in *J. Am. Chem. Soc.* **1958**, *80*, 5507–5513). The solution was stirred at rt for 16 h under an atmosphere of N₂ and then diluted with CH₂Cl₂ (200 mL), washed with satd aq NaHCO₃ (75 mL), brine (75 mL), dried over Na₂SO₄, filtered, and concentrated in vacuo. The crude product was purified via silica gel chromatography eluting with 5% MTBE:CH₂Cl₂ affording the title compound

as a light yellow solid (33.7 g, 88% yield). ¹H NMR (CDCl₃) δ 2.82–2.95 (m, 2H), 2.96–3.07 (m, 3H), 3.07–3.18 (m, 1H), 4.74–4.78 (m, 2H), 6.82 (d, 1H, *J* = 7.6 Hz), 7.37–7.46 (m, 1H), 7.49–7.61 (m, 3H), 7.80–7.95 (m, 3H), 8.16 (br d, 2H, *J* = 6.8 Hz), 8.33 (m, 1H), 8.40 (d, 1H, *J* = 2.3 Hz), 8.63 (d, 1H, *J* = 2.3 Hz). ¹³C NMR (DMSO-*d*₆) δ 32.8, 34.8, 35.0, 54.3, 106.2, 119.0, 126.3, 126.7, 127.2 (2C), 127.7, 128.1, 128.8 (2C), 129.7, 137.0, 138.4, 140.4, 143.1, 143.5, 145.3, 147.3 (2C), 153.5, 156.4, 173.4. MS (ES+): *m/z* 441.09/443.12 (3/1) [MH⁺]. HPLC: *t*_R = 3.74 min (OpenLynx, polar_5 min). Elemental Analysis calcd for C₂₆H₂₁ClN₄O: C, 70.82; H, 4.80; N, 12.71; Cl, 8.04. Found: C, 70.55; H, 4.77; N, 12.52; Cl, 8.26.

General procedure B: synthesis of the 8-chloroimidazopyrazines 8a–8d. A suspension of amide **7** (1.0 equiv) in anhydrous acetonitrile (0.1 M suspension) was charged with POCl₃ (1.4 equiv) dropwise and the reaction mixture was stirred at rt for 5 min prior to the dropwise addition of DMF (0.1 equiv). The reaction mixture was stirred at 55 °C for 2 h. The mixture was concentrated in vacuo, dissolved in CH₂Cl₂, and quenched with 2 N NH₃ in *i*-PrOH to pH 9. The mixture was concentrated in vacuo, dissolved in CH₂Cl₂, washed with water and brine, dried over Na₂SO₄, filtered, and concentrated in vacuo.

4.2.10. 7-(8-Chloro-3-cyclobutylimidazo[1,5-*a*]pyrazin-1-yl)-2-phenylquinoline (8a). The solid was suspended in CHCl₃, filtered, and the filtrate was concentrated in vacuo to obtain the title compound as a yellow solid (89% yield). Mp 214–215 °C. ¹H NMR (CDCl₃) δ 2.04–2.15 (m, 1H), 2.15–2.28 (m, 1H), 2.50–2.60 (m, 2H), 2.64–2.76 (m, 2H), 3.89 (quint, *J* = 8.4 Hz, 1H), 7.35 (d, *J* = 4.8 Hz, 1H), 7.44–7.50 (m, 1H), 7.51–7.57 (m, 3H), 7.89–7.93 (m, 3H), 8.17–8.22 (m, 2H), 8.27 (dd, *J* = 8.8, 0.8 Hz, 1H), 8.53 (d, *J* = 0.8 Hz, 1H). ¹³C NMR (CDCl₃, DEPT135) δ 18.93 (–), 26.84 (2C, –), 31.41 (+), 113.31 (+), 119.26 (+), 120.03 (C_{quart}), 126.52 (+), 126.62 (+), 126.72 (C_{quart}), 127.59 (2C, +), 128.79 (2C, +), 129.14 (+), 129.28 (+), 132.08 (+), 135.06 (C_{quart}), 136.45 (+), 137.26 (C_{quart}), 139.67 (C_{quart}), 144.56 (C_{quart}), 146.08 (C_{quart}), 147.76 (C_{quart}), 157.66 (C_{quart}). MS (ES+): *m/z* 410.9/412.9 (100/39) [MH⁺]. HPLC: *t*_R = 3.7 min (ZQ3, non-polar_5 min). Elemental Analysis calcd for C₂₅H₁₉ClN₄: C, 73.08; H, 4.66; N, 13.63; Cl, 8.63. Found: C, 72.95; H, 4.63; N, 13.57; Cl, 8.80.

4.2.11. 7-(8-Chloro-3-cyclobutylimidazo[1,5-*a*]pyrazin-1-yl)-quinoline (8b). The crude material was adsorbed onto Hydromatrix and chromatographed on silica gel [Jones Flashmaster, 20 g/70 mL cartridge], eluting with hexanes/EtOAc 1:1 → 1:3, yielding the title compound as a yellow foam (93% yield). ¹H NMR (CDCl₃) δ 2.05–2.14 (m, 1H), 2.16–2.28 (m, 1H), 2.50–2.60 (m, 2H), 2.63–2.75 (m, 2H), 3.89 (quint, *J* = 8.4 Hz, 1H), 7.35 (d, *J* = 4.4 Hz, 1H), 7.44 (dd, *J* = 8.2, 4.2 Hz, 1H), 7.55 (d, *J* = 5.2 Hz, 1H), 7.90 (d, *J* = 8.4 Hz, 1H), 8.13 (dd, *J* = 8.4, 1.6 Hz, 1H), 8.22 (d, *J* = 8.2 Hz, 1H), 8.46 (s, 1H), 8.98 (dd, *J* = 4.2, 1.6 Hz, 1H). MS (ES+): *m/z* 335.1/337.1 (100/44) [MH⁺].

4.2.12. 7-(8-Chloro-3-methylimidazo[1,5-*a*]pyrazin-1-yl)-2-phenylquinoline (8c). The title compound was obtained as a light brown oil which was carried forward without further purification (100% yield). ^1H NMR (CDCl_3) δ 2.77 (s, 3H), 7.41–7.59 (m, 4H), 7.70–7.72 (m, 1H), 7.88–7.93 (m, 3H), 8.19–8.28 (br m, 3H), 8.55 (br s, 1H). MS (ES⁺): m/z 370.96/372.97 [MH^+].

4.2.13. 7-[8-Chloro-3-(3-methylenecyclobutyl)imidazo[1,5-*a*]pyrazin-1-yl]-2-phenylquinoline (8d). The crude material was purified via silica gel chromatography eluting with 3–5% $\text{CH}_3\text{CN}/\text{CH}_2\text{Cl}_2$ to afford the desired compound as a yellow solid (93% yield). Mp 211 °C (decomposed). ^1H NMR (CDCl_3) δ 3.23–3.34 (m, 2H), 3.37–3.48 (m, 2H), 3.82–3.95 (m, 1H), 4.90–4.98 (m, 2H), 7.21–7.26 (m, 1H), 7.40 (d, 1H, $J = 5.1$ Hz), 7.46–7.65 (m, 4H), 7.87–8.02 (m, 3H), 8.20–8.30 (m, 2H), 8.40 (br s, 1H). MS (ES⁺): m/z 423.03/423.97 (3/1) [MH^+]. HPLC: $t_R = 3.76$ min (Openlynx, non-polar_5 min). Elemental Analysis calcd for $\text{C}_{26}\text{H}_{19}\text{ClN}_4\text{O} \cdot 1/5\text{H}_2\text{O}$: C, 73.22; H, 4.58; N, 13.14. Found: C, 73.30; H, 4.54; N, 13.05.

4.2.14. Toluene-4-sulfonic acid 3-[8-amino-1-(2-phenylquinolin-7-yl)imidazo[1,5-*a*]pyrazin-3-yl]-cyclobutylmethyl ester (10a and 10b). A dry THF (5 mL) solution of 7-[8-chloro-3-(3-methylenecyclobutyl)imidazo[1,5-*a*]pyrazin-1-yl]-2-phenylquinoline (338 mg, 0.800 mmol), charged with 0.5 M 9-BBN in THF (2.40 mL, 1.20 mmol) dropwise, was stirred at 0 °C under N_2 atmosphere for 30 min and then allowed to warm to rt and stirred for an additional 16 h. The mixture was cooled to 0 °C and charged with 1 N aq NaOH (3 mL) and 30% aq H_2O_2 (0.600 mL). Stirring was continued at 0 °C for 10 min and then at rt for 30 min. The mixture was diluted with CH_2Cl_2 (30 mL), washed with brine (2 × 20 mL), dried over Na_2SO_4 , and filtered. The filtrate was concentrated in vacuo and the crude material was purified by silica gel column chromatography eluting with hexanes/EtOAc (1:1 → 0:1), affording the {3-[8-chloro-1-(2-phenylquinolin-7-yl)imidazo[1,5-*a*]pyrazin-3-yl]-cyclobutyl}-methanol as a mixture of *cis*- and *trans*-isomers in the ratio of 5:1 (220 mg, 62% yield). MS (ES⁺): m/z 441/443 (3/1) [MH^+]. An isopropanol (5 mL) solution of {3-[8-chloro-1-(2-phenylquinolin-7-yl)imidazo[1,5-*a*]pyrazin-3-yl]-cyclobutyl}methanol (265 mg, 0.600 mmol) in a stainless steel Parr apparatus was cooled to –78 °C and charged with NH_3 gas for 1 min. The apparatus was sealed and heated at 110 °C for 3 d, then cooled to –78 °C, vented, and allowed to warm to rt. The salt was removed by filtration and the filtrate was concentrated in vacuo. The crude material was purified via silica gel chromatography eluting with EtOAc → 9:1 EtOAc/MeOH, affording {3-[8-amino-1-(2-phenylquinolin-7-yl)imidazo[1,5-*a*]pyrazin-3-yl]-cyclobutyl}methanol (130 mg, 51% yield) as a mixture of *cis*- and *trans*-isomers in the ratio of 5:1. MS (ES⁺): m/z 422.0 [MH^+]. A suspension of {3-[8-amino-1-(2-phenylquinolin-7-yl)imidazo[1,5-*a*]pyrazin-3-yl]-cyclobutyl}methanol (125 mg, 0.300 mmol) in dry CH_2Cl_2 (5 mL) and pyridine (2.00 mL) was charged with a CH_2Cl_2 (1 mL) solution of Ts_2O (108 mg, 0.330 mmol) at –40 °C under N_2 atmosphere. The mixture was stirred and slowly warmed to rt overnight. The reaction mixture was quenched with water (1 mL), diluted with CH_2Cl_2

(40 mL), washed with satd aq NaHCO_3 (2 × 10 mL) and brine (2 × 10 mL), dried over Na_2SO_4 , filtered, and concentrated in vacuo. The crude material was purified by silica gel column chromatography eluting with EtOAc → 98:2 EtOAc/MeOH → 96:4 EtOAc/MeOH, affording the title compounds **10a** (*cis*) (90 mg, 53% yield) and **10b** (*trans*) (25 mg, 11% yield) as light yellow solids:

4.2.14.1. *cis*-Toluene-4-sulfonic acid 3-[8-amino-1-(2-phenylquinolin-7-yl)imidazo[1,5-*a*]pyrazin-3-yl]-cyclobutylmethyl ester (10a). Mp 177 °C (decomposed). ^1H NMR (CDCl_3) δ 2.30–2.44 (m, 2H), 2.40 (s, 3H), 2.57–2.68 (m, 2H), 2.76–2.90 (m, 1H), 3.71 (quintet, 1H, $J = 8.8$ Hz), 4.11 (d, 2H, $J = 6.6$ Hz), 5.24 (br s, 2H, NH_2), 7.10 and 7.12 (AB, 2H, $J = 5.0$ Hz), 7.30 (d, 2H, $J = 7.8$ Hz), 7.45–7.51 (m, 1H), 7.51–7.57 (m, 2H), 7.75–7.81 (m, 2H), 7.89–8.00 (m, 3H), 8.16–8.22 (m, 2H), 8.28 (d, 1H, $J = 8.6$ Hz), 8.41 (dd, 1H, $J = 0.8, 0.8$ Hz). ^{13}C NMR ($\text{DMSO}-d_6$) δ 21.0, 26.7, 28.7 (2C), 30.1, 73.8, 106.3, 114.1, 118.7, 126.1, 127.2 (2C), 127.5 (2C), 127.89 (2C), 127.92, 128.8 (3C), 129.6, 130.0 (2C), 132.5, 133.2, 136.2, 137.0, 138.6, 143.3, 144.8, 147.5, 151.6, 156.5. MS (ES⁺): m/z 575.98 (50) [MH^+]. HPLC: $t_R = 2.80$ min (OpenLynx, polar_5 min). Elemental Analysis calcd for $\text{C}_{33}\text{H}_{29}\text{N}_5\text{O}_3\text{S}$: C, 68.85; H, 5.08; N, 12.17; S, 5.57. Found: C, 68.81; H, 5.09; N, 12.20; S, 5.47.

4.2.14.2. *trans*-Toluene-4-sulfonic acid 3-[8-amino-1-(2-phenylquinolin-7-yl)imidazo[1,5-*a*]pyrazin-3-yl]-cyclobutylmethyl ester (10b). Mp 179 °C (decomposed). ^1H NMR (CDCl_3) δ 2.33–2.42 (m, 2H), 2.47 (s, 3H), 2.70–2.79 (m, 2H), 2.79–2.91 (m, 1H), 3.76–3.87 (m, 1H), 4.21 (d, $J = 6.0$ Hz, 2H), 5.32 (br s, 2 H), 7.06 and 7.10 (AB, $J = 5.1$ Hz, 2H), 7.38 (d, $J = 8.0$ Hz, 2H), 7.45–7.50 (m, 1H), 7.51–7.57 (m, 2H), 7.83–7.87 (m, 2H), 7.89–7.98 (m, 3H), 8.17–8.21 (m, 2H), 8.27 (d, $J = 8.4$ Hz, 1 H), 8.42 (dd, $J = 0.8, 0.8$ Hz, 1H). ^{13}C NMR (CDCl_3) δ 21.7, 27.7, 28.0 (2C), 30.8, 73.0, 106.4, 114.6, 119.4, 126.6, 127.6 (2C), 127.7, 127.9 (3C), 128.3, 128.9 (2C), 129.5, 129.7, 129.9 (2C), 133.2, 134.7, 136.2, 136.6, 139.4, 143.7, 144.9, 148.2, 151.5, 158.1. MS (ES⁺): m/z 576.08 (50) [MH^+]. HPLC: $t_R = 2.88$ min (ZQ3, polar_5 min). Elemental Analysis calcd for $\text{C}_{33}\text{H}_{29}\text{N}_5\text{O}_3\text{S}$: C, 68.85; H, 5.08; N, 12.17; S, 5.57. Found: C, 68.59; H, 5.09; N, 11.95; S, 5.55.

General procedure C: synthesis of 8-aminoimidazopyrazines 2a–2c. Ammonia (g) was bubbled into a 0.1 M slurry of the 8-chloroimidazopyrazine **8** in 2 M NH_3 in *i*-PrOH for 8 min in a stainless steel Parr apparatus cooled to –78 °C in a dry ice/acetone bath. The Parr apparatus was secured and the cooling bath was removed. The reaction mixture was heated at 110 °C for 24 h, then cooled to –78 °C, vented, and allowed to warm to rt. The reaction mixture was transferred to a round bottom flask and the solvent was concentrated in vacuo. The product was resuspended in CH_2Cl_2 and the remaining salts were removed by filtration and the filtrate was concentrated in vacuo.

4.2.15. 3-Cyclobutyl-1-(2-phenylquinolin-7-yl)imidazo[1,5-*a*]pyrazin-8-ylamine (2a). The crude material was chromatographed on silica gel [Jones Flashmaster, 10 g/70 mL

cartridge], eluting with $\text{CH}_2\text{Cl}_2 \rightarrow 1\%$ MeOH in $\text{CH}_2\text{Cl}_2 \rightarrow 2\%$ MeOH in CH_2Cl_2 , giving the desired product as a yellow solid (73% yield). Mp 184–186 °C. ^1H NMR (CDCl_3) δ 2.01–2.12 (m, 1H), 2.13–2.27 (m, 1H), 2.47–2.58 (m, 2H), 2.62–2.73 (m, 2H), 3.85 (quint, $J = 8.0$ Hz, 1H), 6.00 (br s, 2H), 7.04 (d, $J = 5.4$ Hz, 1H), 7.15 (d, $J = 5.4$ Hz, 1H), 7.46–7.51 (m, 1H), 7.52–7.58 (m, 2H), 7.91 (dd, $J = 8.4, 1.6$ Hz, 1H), 7.94 (d, $J = 8.4$ Hz, 1H), 7.97 (d, $J = 8.0$ Hz, 1H), 8.18–8.22 (m, 2H), 8.28 (d, $J = 8.4$ Hz, 1H), 8.42 (d, $J = 0.8$ Hz, 1H). ^{13}C NMR (CDCl_3 , DEPT135) δ 18.89 (–), 26.92 (2C, –), 31.50 (+), 106.62 (+), 114.32 (C_{quart}), 119.26 (+), 126.55 (C_{quart}), 127.56 (3C, +), 128.06 (+), 128.15 (+), 128.83 (2C, +), 129.44 (+), 129.67 (+), 134.56 (C_{quart}), 136.42 (C_{quart}), 136.53 (+), 139.44 (C_{quart}), 144.40 (C_{quart}), 148.18 (C_{quart}), 151.62 (C_{quart}), 157.94 (C_{quart}). MS (ES+): m/z 392.0 (50) [MH^+]. HPLC: $t_{\text{R}} = 1.7$ min (OpenLynx, non-polar_5 min), 2.5 min (ZQ3, polar_5 min). Elemental Analysis calcd for $\text{C}_{25}\text{H}_{21}\text{N}_5 \cdot 0.4\text{H}_2\text{O}$: C, 75.32; H, 5.51; N, 17.57. Found: C, 75.22; H, 5.28; N, 17.46. HRMS (ES+) for $\text{C}_{25}\text{H}_{21}\text{N}_5\text{H}^+$ [MH^+]: calcd, 392.1870; found, 392.1890.

4.2.16. 3-Cyclobutyl-1-quinolin-7-ylimidazo[1,5-*a*]pyrazin-8-ylamine (2b). The crude material was adsorbed onto Hydromatrix and chromatographed on silica gel [Jones Flashmaster, 10 g/70 mL cartridge], eluting with $\text{CH}_2\text{Cl}_2 \rightarrow 2\%$ MeOH in $\text{CH}_2\text{Cl}_2 \rightarrow 4\%$ MeOH in $\text{CH}_2\text{Cl}_2 \rightarrow 5\%$ MeOH in $\text{CH}_2\text{Cl}_2 \rightarrow 7\%$ MeOH in CH_2Cl_2 , yielding the title compound as a yellow solid (90% yield). Mp 94–96 °C. ^1H NMR (CDCl_3) δ 2.00–2.10 (m, 1H), 2.12–2.25 (m, 1H), 2.47–2.57 (m, 2H), 2.61–2.73 (m, 2H), 3.85 (quint, $J = 8.4$ Hz, 1H), 5.23 (br s, 2H), 7.10 (d, $J = 4.4$ Hz, 1H), 7.16 (d, $J = 4.4$ Hz, 1H), 7.44 (dd, $J = 8.2, 4.2$ Hz, 1H), 7.95 (d, $J = 8.4$ Hz, 1H), 8.00 (d, $J = 8.4$ Hz, 1H), 8.22 (d, $J = 8.2$ Hz, 1H), 8.36 (s, 1H), 8.95–9.00 (m, 1H). ^{13}C NMR ($\text{DMSO}-d_6$, DEPT135) δ 18.31 (–), 26.54 (2C, +), 30.57 (+), 106.41 (+), 114.03 (C_{quart}), 121.50 (+), 127.05 (C_{quart}), 127.89 (+), 128.09 (+), 128.22 (+), 128.61 (+), 133.04 (C_{quart}), 135.85 (+), 135.92 (C_{quart}), 143.85 (C_{quart}), 147.66 (C_{quart}), 151.03 (+), 151.66 (C_{quart}). MS (ES+): m/z 316.2 (30) [MH^+]. HPLC: $t_{\text{R}} = 1.9$ min (ZQ3, polar_5 min). Elemental Analysis calcd for $\text{C}_{25}\text{H}_{21}\text{N}_5 \cdot 1/12 \text{CH}_2\text{Cl}_2 \cdot 1/12 \text{hexane}$: C, 71.36; H, 5.61; N, 21.25. Found: C, 71.53; H, 5.69; N, 21.11.

4.2.17. 3-Methyl-1-(2-phenylquinolin-7-yl)-imidazo[1,5-*a*]pyrazin-8-ylamine (2c). The compound was purified by silica gel column chromatography [Jones Flashmaster, 10 g cartridge], eluting with 1% MeOH/EtOAc, yielding the title compound as a dark yellow solid (24% yield). ^1H NMR (CDCl_3) δ 2.71 (s, 3H), 5.61 (br s, 2H), 7.13 (d, 1H, $J = 5.1$ Hz), 7.20 (d, 1H, $J = 5.1$ Hz), 7.48–7.56 (m, 3H), 7.89–7.97 (m, 3H), 8.18–8.21 (m, 2H), 8.27 (d, 1H, $J = 8.6$ Hz), 8.39 (s, 1H). ^{13}C NMR (CDCl_3 , DEPT135) δ 12.47 (+), 106.43 (+), 114.31 (C_{quart}), 119.34 (+), 126.58 (C_{quart}), 127.56 (2C, +), 127.86 (+), 127.93 (+), 128.21 (+), 128.84 (2C, +), 129.42 (+), 129.48 (+), 134.63 (C_{quart}), 136.15 (C_{quart}), 136.57 (+), 137.82 (C_{quart}), 139.38 (C_{quart}), 148.13 (C_{quart}), 151.52 (C_{quart}), 158.00 (C_{quart}). MS (ES+): m/z 352.06 [MH^+]. HPLC: $t_{\text{R}} = 2.2$ min (ZQ3, polar_5 min). HRMS (ES+)

for $\text{C}_{22}\text{H}_{17}\text{N}_5\text{H}^+$ [MH^+]: calcd, 352.1557; found, 352.1559.

General procedure D: synthesis of aminomethylcyclobutyl-derived imidazopyrazines 2d–i. A sealed tube containing a solution of toluene-4-sulfonic acid 3-[8-amino-1-(2-phenylquinolin-7-yl)imidazo[1,5-*a*]pyrazin-3-yl]cyclobutylmethyl ester **10** (0.15 mmol) in THF (3.0 mL) was charged with amine (3.6 mmol), sealed, and heated at 50 °C for 16 h. The mixture was concentrated in vacuo to afford the crude product.

4.2.18. *cis*-3-{3-[(Dimethylamino)methyl]cyclobutyl}-1-(2-phenylquinolin-7-yl)imidazo[1,5-*a*]pyrazin-8-ylamine (2d). The crude material was purified by mass-directed HPLC purification to afford the title compound as a light yellow solid (57% yield). ^1H NMR (CDCl_3) δ 2.26 (s, 6H), 2.29–2.40 (m, 2H), 2.45 (d, $J = 6.3$ Hz, 2H), 2.61–2.75 (m, 3H), 3.65–3.76 (m, 1H), 5.18 (br s, 2H), 7.11 (d, $J = 5.1$ Hz, 1H), 7.19 (d, $J = 5.1$ Hz, 1H), 7.46–7.52 (m, 1H), 7.52–7.59 (m, 2H), 7.91–7.99 (m, 3H), 8.18–8.23 (m, 2H), 8.28 (d, $J = 8.8$ Hz, 1H), 8.43 (s, 1H). MS (ES+): m/z 449.34 (100) [MH^+]. HPLC: $t_{\text{R}} = 1.76$ min (OpenLynx, polar_5 min). HRMS (ES+) for $\text{C}_{28}\text{H}_{28}\text{N}_6\text{H}^+$ [MH^+]: calcd, 449.2449; found, 449.2444.

4.2.19. *trans*-3-{3-[(Dimethylamino)methyl]cyclobutyl}-1-(2-phenylquinolin-7-yl)imidazo[1,5-*a*]pyrazin-8-ylamine (2e). The crude material was purified by silica gel column chromatography [Jones Flashmaster, 5 g cartridge], eluting with 5% 7 N NH_3 in MeOH/ CH_2Cl_2 , to afford the title compound as a yellow solid (86% yield). ^1H NMR (CDCl_3) δ 2.27 (s, 6H), 2.28–2.36 (m, 2H), 2.55 (d, $J = 6.8$ Hz, 2H), 2.73–2.84 (m, 3H), 3.80–3.90 (m, 1H), 5.20 (br s, 2H), 7.09–7.14 (m, 2H), 7.45–7.52 (m, 1H), 7.52–7.59 (m, 2H), 7.93 (d, $J = 8.6$ Hz, 1H), 7.97 (s, 2H), 8.18–8.23 (m, 2H), 8.28 (d, $J = 8.6$ Hz, 1H), 8.45 (s, 1H). MS (ES+): m/z 449.37 (100) [MH^+]. HPLC: $t_{\text{R}} = 1.78$ min (OpenLynx, polar_5 min). HRMS (ES+) for $\text{C}_{28}\text{H}_{28}\text{N}_6\text{H}^+$ [MH^+]: calcd, 449.2449; found, 449.2448.

4.2.20. *cis*-3-(3-Azetidin-1-ylmethylcyclobutyl)-1-(2-phenylquinolin-7-yl)imidazo[1,5-*a*]pyrazin-8-ylamine (2f). The crude material was purified by mass-directed HPLC purification to afford the title compound as a light yellow solid (75% yield). Mp 161 °C (decomposed). ^1H NMR (CDCl_3) δ 2.03–2.16 (m, 2H), 2.27–2.38 (m, 2H), 2.46–2.59 (m, 3H), 2.59–2.70 (m, 2H), 3.25 (t, $J = 7.1$ Hz, 4H), 3.68–3.78 (m, 1H), 5.19 (br s, 2H, NH_2), 7.11 (d, $J = 5.1$ Hz, 1H), 7.18 (d, $J = 4.8$ Hz, 1H), 7.46–7.51 (m, 1H), 7.52–7.59 (m, 2H), 7.89–7.99 (m, 3H), 8.15–8.23 (m, 2H), 8.28 (d, $J = 8.5$ Hz, 1H), 8.43 (s, 1H). ^{13}C NMR ($\text{DMSO}-d_6$) δ 17.6, 27.5, 30.3, 31.6 (2C), 54.9 (2C), 64.9, 106.4, 114.0, 118.7, 126.1, 127.2 (2C), 127.9, 128.0, 128.8, 128.87 (2C), 128.93, 129.7, 133.1, 136.3, 137.0, 138.6, 143.8, 147.5, 151.7, 156.5. MS (ES+): m/z 461.06 (90) [MH^+]. HPLC: $t_{\text{R}} = 1.97$ min (OpenLynx, polar_5 min). Elemental Analysis calcd for $\text{C}_{29}\text{H}_{28}\text{N}_6 \cdot 1.75 \text{H}_2\text{O}$: C, 70.78; H, 6.45; N, 17.08. Found: C, 70.59; H, 6.22; N, 17.06. HRMS (ES+) for $\text{C}_{29}\text{H}_{28}\text{N}_6\text{H}^+$ [MH^+]: calcd, 461.2449; found, 461.2431.

4.2.21. trans-3-(3-Azetidin-1-ylmethylcyclobutyl)-1-(2-phenylquinolin-7-yl)imidazo[1,5-a]pyrazin-8-ylamine (2g).

The mixture was concentrated in vacuo and the residue was purified by mass-directed HPLC purification to afford the title compound as a light yellow solid (13% yield). $^1\text{H NMR}$ (CDCl_3) δ 2.11 (quintet, $J = 7.0$ Hz, 2H), 2.34–2.25 (m, 2H), 2.63–2.50 (m, 1H), 2.67 (d, $J = 7.4$ Hz, 2H), 2.79–2.70 (m, 2H), 3.26 (t, $J = 6.8$ Hz, 4H), 3.86–3.77 (m, 1H), 5.20 (br s, 2H), 7.10 (s, 2H), 7.50–7.45 (m, 1H), 7.57–7.51 (m, 2H), 7.92 (d, $J = 8.6$ Hz, 1H), 7.97–7.94 (m, 2H), 8.22–8.18 (m, 2H), 8.27 (dd, $J = 8.6, 0.6$ Hz, 1H), 8.43 (d, $J = 1.0$ Hz, 1H). MS (ES+): m/z 461 (100) [MH^+]. HPLC: $t_{\text{R}} = 1.81$ min (OpenLynx, polar_5 min).

4.2.22. cis-3-[3-(Morpholin-4-ylmethyl)cyclobutyl]-1-(2-phenylquinolin-7-yl)imidazo[1,5-a]pyrazin-8-ylamine (2h).

The crude material was purified by mass-directed HPLC purification to afford the title compound as a light yellow solid (69% yield). $^1\text{H NMR}$ (CDCl_3) δ 2.31–2.41 (m, 2H), 2.43–2.50 (m, 4H), 2.54 (d, $J = 6.1$ Hz, 2H), 2.64–2.74 (m, 3H), 3.66–3.75 (m, 5H), 5.19 (br s, 2H), 7.12 (d, $J = 5.1$ Hz, 1H), 7.18 (d, $J = 5.1$ Hz, 1H), 7.46–7.52 (m, 1H), 7.52–7.59 (m, 2H), 7.91–7.97 (m, 3H), 8.17–8.22 (m, 2H), 8.28 (d, $J = 8.6$ Hz, 1H), 8.43 (s, 1H). MS (ES+): m/z 491 (100) [MH^+]. HPLC: $t_{\text{R}} = 1.78$ min (OpenLynx, polar_5 min). HRMS (ES+) for $\text{C}_{30}\text{H}_{30}\text{N}_6\text{O}\cdot\text{H}^+$ [MH^+]: calcd, 491.2554; found, 491.2547.

4.2.23. trans-3-[3-(Morpholin-4-ylmethyl)cyclobutyl]-1-(2-phenylquinolin-7-yl)imidazo[1,5-a]pyrazin-8-ylamine (2i).

The crude material was purified by preparative TLC eluting with 1% MeOH:EtOAc followed by recrystallization from EtOAc/Hexanes to afford the title compound as a yellow solid (66% yield). $^1\text{H NMR}$ (CDCl_3) δ 2.28–2.38 (m, 2H), 2.44–2.50 (m, 4H), 2.62 (d, $J = 6.8$ Hz, 2H), 2.72–2.87 (m, 3H), 3.69–3.75 (m, 4H), 3.78–3.89 (m, 1H), 5.24 (br s, 2H), 7.11 (s, 2H), 7.45–7.52 (m, 1H), 7.52–7.58 (m, 2H), 7.94 (d, $J = 8.6$ Hz, 1H), 7.95–7.98 (m, 2H), 8.17–8.23 (m, 2H), 8.29 (d, $J = 8.6$ Hz, 1H), 8.45 (s, 1H). MS (ES+): m/z 491.37 (100) [MH^+]. HPLC: $t_{\text{R}} = 1.78$ min (OpenLynx, polar_5 min). HRMS (ES+) for $\text{C}_{30}\text{H}_{30}\text{N}_6\text{O}\cdot\text{H}^+$ [MH^+]: calcd, 491.2554; found, 491.2553.

4.2.24. 3-[8-Chloro-1-(2-phenylquinolin-7-yl)imidazo[1,5-a]pyrazin-3-yl]cyclobutanone (11). A solution of 7-[8-chloro-3-(3-methylenecyclobutyl)imidazo[1,5-a]pyrazin-1-yl]-2-phenylquinoline (20.0 g, 47.3 mmol) in THF (600 mL) was charged with NMO (6.09 g, 0.520 mol), potassium osmate dihydrate (0.870 g, 0.002 mol), and water (200 mL). The reaction mixture was stirred at rt for 20 h and then quenched with excess Na_2SO_3 . After stirring for an additional 10 min, the mixture was diluted with EtOAc (400 mL) and washed with brine (2×250 mL). The organic phase was passed through Celite, dried over Na_2SO_4 , filtered, and concentrated in vacuo to afford the desired compound as a yellow solid (24.5 g). The crude material (24.0 g, 47.3 mmol) in THF (600 mL) and water (200 mL) was charged with NaIO_4 at 0 °C and the mixture was allowed to warm to rt and stirred for 4 h. The mixture was diluted with EtOAc (400 mL) and washed with brine (2×150 mL).

The combined organic phases were dried over Na_2SO_4 , filtered, and concentrated in vacuo. The crude material was purified via silica gel chromatography eluting with 3 → 5% MeOH: CH_2Cl_2 to afford the desired compound as a yellow solid (17.7 g, 88% yield in two steps). Mp 250 °C (decomposed). $^1\text{H NMR}$ (CDCl_3) δ 3.63–3.71 (m, 2H), 3.85–3.99 (m, 3H), 7.44–7.56 (m, 4H), 7.65 (d, $J = 4.8$ Hz, 1H), 7.90–7.95 (m, 3H), 8.22 (d, $J = 8.0$ Hz, 2H), 8.32 (d, $J = 8.8$ Hz, 1H), 8.61 (s, 1H). $^{13}\text{C NMR}$ ($\text{DMSO}-d_6$) δ 19.9, 52.2 (2C), 115.3, 119.1, 119.8, 126.4 (2C), 126.9, 127.2 (2C), 128.8 (2C), 129.0, 129.6, 130.9, 134.9, 135.2, 137.0, 138.5, 143.4, 143.7, 146.9, 156.6, 205.5. MS (ES+): m/z 425.04/427.06 (3/1) [MH^+]. HPLC: $t_{\text{R}} = 2.38$ min (ZQ3, non-polar_5 min). Elemental Analysis calcd for $\text{C}_{25}\text{H}_{17}\text{ClN}_4\text{O}\cdot 0.2\text{H}_2\text{O}$: C, 70.08; H, 4.09; N, 13.08. Found: C, 70.10; H, 4.02; N, 12.88.

General procedure E: synthesis of 3-aminocyclobutyl-derived imidazopyrazines 2j–o from 3-[8-chloro-1-(2-phenylquinolin-7-yl)imidazo[1,5-a]pyrazin-3-yl]cyclobutanone (11). A solution of 3-[8-chloro-1-(2-phenylquinolin-7-yl)imidazo[1,5-a]pyrazin-3-yl]cyclobutanone (0.234 mmol) and amine (0.200 mmol) in DCE (5 mL) was charged with sodium triacetoxyborohydride (0.468 mmol). The resulting mixture was stirred at rt for 16 h. The reaction mixture was diluted with CH_2Cl_2 , washed with NaHCO_3 , brine, dried over Na_2SO_4 , filtered, and then concentrated in vacuo, affording the desired product as a yellow solid, which was carried forward without further purification. Ammonia (g) was bubbled into a 0.1 M slurry of the 8-chloroimidazopyrazine in 2 M NH_3 in *i*-PrOH for 8 min in a stainless steel Parr apparatus cooled to -78 °C in a dry ice/acetone bath. The Parr apparatus was secured and the cooling bath was removed. The reaction mixture was heated at 110 °C for 24 h, then cooled to -78 °C, vented, and allowed to warm to rt. The reaction mixture was concentrated in vacuo and the residue was suspended in CH_2Cl_2 . The remaining salts were removed by filtration and the filtrate was concentrated in vacuo.

4.2.25. cis-3-[3-(Dimethylamino)cyclobutyl]-1-(2-phenylquinolin-7-yl)imidazo[1,5-a]pyrazin-8-ylamine (2j).

The product was submitted to mass-directed HPLC purification to afford the title compound as a yellow solid (54% yield). $^1\text{H NMR}$ (CDCl_3) δ 2.23 (s, 6H), 2.54 (m, 2H), 2.69 (m, 2H), 2.90 (m, 1H), 3.45 (m, 1H), 5.27 (br s, 2H), 7.11 (d, $J = 4.8$ Hz, 1H), 7.21 (d, $J = 4.8$ Hz, 1H), 7.47–7.56 (m, 3H), 7.91–7.94 (m, 3H), 8.18–8.20 (m, 2H), 8.27 (d, $J = 8.8$ Hz, 1H), 8.39 (s, 1H). MS (ES+): m/z 435 [MH^+]. HPLC: $t_{\text{R}} = 2.28$ min (ZQ3, polar_5 min). HRMS (ES+) for $\text{C}_{27}\text{H}_{26}\text{N}_6\cdot\text{H}^+$ [MH^+]: calcd, 435.2292; found, 435.2292.

4.2.26. cis-3-((3-Azetidin-1-yl)-cyclobutyl)-1-(2-phenylquinolin-7-yl)imidazo[1,5-a]pyrazin-8-ylamine (2k).

The crude material was purified by silica gel column chromatography eluting with 5% 2 M NH_3 in MeOH/ CH_2Cl_2 to afford the title compound as a yellow solid (71% yield). $^1\text{H NMR}$ (CDCl_3) δ 2.05–2.09 (m, 2H), 2.50–2.60 (m, 4H), 3.25–3.29 (m, 6H), 5.20 (br s, 2H), 7.11 (d, $J = 5.2$ Hz, 1H), 7.19 (d, $J = 5.2$ Hz, 1H), 7.48–7.57 (m, 3H), 7.91–7.95 (m, 3H), 8.18–8.20 (m, 2H), 8.27

(d, $J = 8.4$ Hz, 1H), 8.41 (s, 1H). MS (ES+): m/z 447.10 [MH⁺]. HPLC: $t_R = 1.76$ min (Open Lynx, polar_5 min). HRMS (ES+) for C₂₈H₂₆N₆H⁺ [MH⁺]: calcd, 447.2292; found, 447.2309.

4.2.27. cis-3-[3-(Pyrrolidine)cyclobutyl]-1-(2-phenylquinolin-7-yl)imidazo[1,5-*a*]pyrazin-8-ylamine (2l). The product was submitted to mass-directed HPLC purification to afford the title compound as a yellow solid (18% yield). ¹H NMR (CDCl₃) δ 1.80 (m, 4H), 2.54–2.69 (m, 8H), 3.15 (m, 1H), 3.5 (m, 1H), 5.23 (br s, 2H), 7.10 (d, $J = 4.4$ Hz, 1H), 7.19 (d, $J = 4.8$ Hz, 1H), 7.47–7.55 (m, 3H), 7.90–7.94 (m, 3H), 8.19 (m, 2H), 8.26 (d, $J = 8.0$ Hz, 1H), 8.39 (s, 1H). MS (ES+): m/z 461.3 [MH⁺]. HPLC: $t_R = 1.84$ min (OpenLynx, polar_5 min). HRMS (ES+) for C₂₉H₂₈N₆H⁺ [MH⁺]: calcd, 461.2449; found, 461.2426.

4.2.28. cis-1-(2-Phenylquinolin-7-yl)-3-(3-piperidin-1-ylcyclobutyl)imidazo[1,5-*a*]pyrazin-8-ylamine (2m). The crude material was purified by recrystallization from CH₂Cl₂/Hexanes (4:1) to afford the title compound as a yellow solid (37% yield). ¹H NMR (CDCl₃) δ 1.45–1.46 (m, 2H), 1.57–1.62 (m, 4H), 2.31–2.39 (m, 4H), 2.50–2.55 (m, 2H), 2.65–2.72 (m, 2H), 2.88 (m, 1H), 3.47 (m, 1H), 5.22 (br s, 2H), 7.10 (d, $J = 4.8$ Hz, 1H), 7.20 (d, $J = 5.2$ Hz, 1H), 7.47–7.56 (m, 3H), 7.91–7.94 (m, 3H), 8.18–8.21 (m, 2H), 8.26 (d, $J = 8.4$ Hz, 1H), 8.38 (s, 1H). MS (ES+): m/z 475.10 [MH⁺]. HPLC: $t_R = 1.83$ min (OpenLynx, polar_5 min). HRMS (ES+) for C₃₀H₃₀N₆H⁺ [MH⁺]: calcd, 475.2605; found, 475.2605.

4.2.29. cis-1-(2-Phenylquinolin-7-yl)-3-(3-thiomorpholin-4-ylcyclobutyl)imidazo[1,5-*a*]pyrazin-8-ylamine (2n). The crude material was purified by recrystallization from EtOAc/Hexanes (4:1) to afford the title compound as a yellow solid (60% yield). Mp 145–150 °C (decomposed). ¹H NMR (CDCl₃) δ 2.43–2.51 (m, 2H), 2.64–2.73 (m, 10H), 2.94–2.98 (m, 1H), 3.45–3.50 (m, 1H), 5.24 (br s, 2H), 7.11 (d, $J = 5.2$ Hz, 1H), 7.19 (d, $J = 5.2$ Hz, 1H), 7.46–7.57 (m, 3H), 7.91–7.97 (m, 3H), 8.18–8.21 (m, 2H), 8.27 (d, $J = 8.8$ Hz, 1H), 8.40 (s, 1H). ¹³C NMR (DMSO-*d*₆, DEPT135) δ 23.14 (+), 26.90 (2C, –), 32.19 (2C, –), 50.52 (2C, –), 56.03 (+), 106.42 (+), 114.05 (C_{quart}), 118.75 (+), 126.15 (C_{quart}), 127.22 (2C, +), 127.93 (2C, +), 127.99 (+), 128.81 (+), 128.88 (2C, +), 129.67 (+), 133.26 (C_{quart}), 136.24 (C_{quart}), 137.04 (+), 138.59 (C_{quart}), 143.44 (C_{quart}), 147.53 (C_{quart}), 151.66 (C_{quart}), 156.51 (C_{quart}). MS (ES+): m/z 493.08 [MH⁺]. HPLC: $t_R = 1.92$ min (ZQ3, polar_5 min). Elemental Analysis calcd for C₂₉H₂₈N₆S·0.2H₂O·0.2 hexane: C, 70.64; H, 6.12; N, 16.37. Found: C, 70.33; H, 5.94; N, 16.29. HRMS (ES+) for C₂₉H₂₈N₆S·H⁺ [MH⁺]: calcd, 493.2169; found, 493.2182.

4.2.30. cis-3-(3-Morpholin-4-ylcyclobutyl)-1-(2-phenylquinolin-7-yl)imidazo[1,5-*a*]pyrazin-8-ylamine (2o). The product was submitted to mass-directed HPLC purification to afford the title compound as a yellow solid (45% yield). Mp 230–235 °C (decomposed). ¹H NMR (CDCl₃) δ 2.37–2.47 (m, 4H), 2.47–2.57 (m, 2H), 2.64–

2.73 (m, 2H), 2.91–3.01 (m, 1H), 3.45–3.56 (m, 1H), 3.70–3.79 (m, 4H), 5.23 (br s, 2H), 7.12 (d, $J = 4.8$ Hz, 1H), 7.20 (d, $J = 4.8$ Hz, 1H), 7.45–7.59 (m, 3H), 7.90–7.98 (m, 3H), 8.17–8.23 (m, 2H), 8.27 (d, $J = 8.4$ Hz, 1H), 8.40 (s, 1H). ¹³C NMR (DMSO-*d*₆, DEPT135) δ 23.25 (+), 31.63 (2C, –), 49.37 (2C, –), 56.12 (+), 65.98 (2C, –), 106.41 (+), 114.04 (C_{quart}), 118.74 (+), 126.13 (C_{quart}), 127.21 (2C, +), 127.91 (2C, +), 127.97 (+), 128.78 (+), 128.86 (2C, +), 129.64 (+), 133.23 (C_{quart}), 136.24 (C_{quart}), 137.02 (+), 138.57 (C_{quart}), 143.46 (C_{quart}), 147.51 (C_{quart}), 151.64 (C_{quart}), 156.49 (C_{quart}). MS (ES+): m/z 477.30 [MH⁺]. HPLC: $t_R = 1.75$ min (Open Lynx, polar_5 min); 1.86 min (ZQ3, polar_5 min). HRMS (ES+) for C₂₉H₂₈N₆O·H⁺ [MH⁺]: calcd, 477.2398; found, 477.2408.

4.2.31. 3-Cyclobutyl-1-(2-phenylquinolin-7-yl)imidazo[1,5-*a*]pyrazin-8-ol (9). A THF (2.0 mL) solution of 7-(8-chloro-3-cyclobutyl-2*H*-imidazo[1,5-*a*]pyrazin-1-yl)-2-phenylquinoline (50 mg, 0.12 mmol) was charged with water (2 mL) and 37% HCl (2 mL) and heated at 60 °C for 30 min. The solution was allowed to cool to rt and stirred for 16 h. THF was removed in vacuo and the aqueous solution was treated with 5 N NaOH until pH 10 was achieved. The resulting solid was filtered, washed with water (2 × 5 mL), and dried in vacuo to afford 45 mg of the title compound as a yellow solid (94% yield). ¹H NMR (DMSO-*d*₆) δ 1.91–2.02 (m, 1H), 2.10 (quintet, $J = 9.2$ Hz, 1H), 2.39–2.50 (m, 4H), 3.96 (quintet, $J = 8.4$ Hz, 1H), 6.70 (dd, $J = 5.6, 5.6$ Hz, 1H), 7.22 (d, $J = 5.6$ Hz, 1H), 7.49–7.62 (m, 3H), 8.00 (d, $J = 8.8$ Hz, 1H), 8.13 (d, $J = 8.8$ Hz, 1H), 8.30 (d, $J = 6.8$ Hz, 2H), 8.44 (d, $J = 8.4$ Hz, 1H), 8.59 (d, $J = 8.4$ Hz, 1H), 9.11 (s, 1H), 10.71 (d, $J = 2.8$ Hz, 1H). MS (ES+): m/z 393 (100) [MH⁺].

4.3. Biological evaluation

4.3.1. Cell lines. 3T3/huIGFIR cells, derived from NIH 3T3 cells stably overexpressing full-length human IGF-IR, were obtained from Dr. J. Beebe (Pfizer, Inc.). GEO human cancer cells were kindly provided from Dr. M. Brattain (Roswell Park Cancer Institute) and were maintained in McCoy's 5A medium supplemented with 10% FCS and 1% L-glutamine or in serum-free conditioned culture system. MCF-7, NCI-H292, Colo-699, NCI-H358, HT-29, Colo-205, and HepG2 cells were from ATCC (Manassas, VA) and cultured in the appropriate media according to ATCC recommendations.

4.3.2. Antibodies. The following antibodies were used for immunoprecipitation or as the capture antibody in ELISAs: human IGF-IR (Ab-1, Calbiochem, EMD, CA) and IR (Ab-2, Lab Vision Corp., CA) for capture; human IGF-IR β (sc-713, Santa Cruz Biotechnology) for immunoprecipitation. The following antibodies were used for immunoblotting analysis: human IGF-IR β (sc-713, Santa Cruz Biotechnology), antiphosphotyrosine (X1021, Exalpa Biologicals, MA), antiphosphotyrosine-horseradish peroxidase (HRP) conjugate (mouse anti-Phosphotyrosine-HRP, Invitrogen-ZYMED), pAKT⁴⁷³ (9271, Cell Signaling Technology), p-p70S6K (9205, Cell Signaling Technology), and GAPDH (9482, Abcam).

4.3.3. Protein kinase biochemical assays. Protein kinase assays were either performed in-house by ELISA-based assay methods (IGF-IR, IR, Kit, EGFR, and KDR) or at Upstate Inc. (Charlottesville, VA) by a radiometric method (KinaseProfiler service). In-house ELISAs used poly(Glu:Tyr) (Sigma, St. Louis, MO) as the substrate bound to the surface of 96-well assay plates, and phosphorylation was detected using an antiphosphotyrosine antibody conjugated to HRP. The bound antibody was quantified using ABTS as the peroxidase substrate by measuring absorbance at 405/490 nm. All assays used purified recombinant kinase catalytic domains. Recombinant enzymes of human IGF-IR or EGFR were expressed as an NH₂-terminal glutathione *S*-transferase fusion protein in insect cells and were purified in-house. The human IR protein was purchased from Calbiochem (Cat# 407697). IC₅₀ values were determined from the sigmoidal dose–response plot of percent inhibition versus log₁₀ compound concentration (Xlfit 3.0, IDBS). A minimum of three measurements, performed in duplicate, were carried out with in-house assays unless otherwise indicated.

4.3.4. Protein kinase inhibition in intact cells. Quantitative 96-well ELISAs were developed to study the cellular effects of AQIP. Cells were placed into 96-well plates in media containing low serum (0.5% FCS) at 37 °C for 2 h (3T3/huIGFIR) or overnight (HepG2), and then were treated with various concentrations of compound for 2 h before lysis (the final DMSO concentration in the assay was 0.4%), and the appropriate ligand was added for the final 15 min of the compound treatment period (100 ng/mL IGF-I, R&D systems or 10 ng/mL insulin, Roche). Lysates were prepared in TGH buffer⁴⁷ (1% Triton-100, 10% glycerol, 50 mmol/L Hepes, pH 7.4) supplemented with 150 mmol/L NaCl, 1.5 mmol/L MgCl₂, 1 mmol/L EDTA, and fresh protease and phosphatase inhibitors (10 µg/mL leupeptin, 25 µg/mL aprotinin, and 200 µmol/L Na₃VO₄). ELISAs of the target protein phosphorylation were done by transferring lysates into a second 96-well plate that was precoated with the appropriate capture antibody. The target proteins were then probed with an antiphosphotyrosine antibody-HRP conjugate using a chemiluminescent HRP substrate (Pierce) for detection by luminometry.

For immunoblotting analysis, lysates were cleared of insoluble material by centrifugation at 15,000g for 5 min at 4 °C and the resultant supernatant was subjected to immunoprecipitation with anti-IGF-IR antibody (sc-713) coupled to Protein G–Sepharose beads (Sigma, St. Louis, MO), followed by SDS–PAGE and immunoblotting with antiphosphotyrosine antibody-HRP conjugate and chemiluminescent detection. Alternatively, for highly abundant protein targets (IGF-IR, pErk1/2, pAkt, and p-p70S6K), lysates were analyzed directly by SDS–PAGE and immunoblotting.

4.3.5. Cell proliferation and DNA fragmentation. For assays of cell proliferation, cells were seeded into 96-well plates in appropriate media containing 10% FCS and incubated for 3 d in the presence of AQIP at various concentrations. Inhibition of cell growth was deter-

mined by luminescent quantitation of intracellular ATP content using CellTiterGlo (Promega, Madison, WI).

For assay of DNA fragmentation, 5 × 10³ cells per well were seeded in a 96-well plate and treated with AQIP at 10 µM for 48 h in the presence of 10% FCS. DNA fragments were detected using Cell Death Detection ELISA^{PLUS} (Cat#11774425001), according to the instructions provided by the manufacturer. Data were expressed as fold of DNA induction over the DMSO control cells.

4.3.6. Metabolic stability assay. Compound was mixed with microsomes of human and mouse, and the reaction was initiated by the addition of NADPH for 0 (pre-NADPH addition), 5, 10, 20 or 40 min. The reactions were terminated with chilled methanol. After centrifugation to precipitate protein, supernatants were analyzed by LC–MS/MS. Various pharmacokinetic parameters were calculated, including half-life (*t*_{1/2}), intrinsic clearance (Cl_{int}), and scaled hepatic clearance (Cl_h), dependent upon the species. An ‘Extraction Ratio’ (ER) was calculated by the formula ER = Cl_h/hepatic blood flow.

4.3.7. Cytochrome P450 3A4 assay. Cytochrome P450 3A4 activity was measured using P450-Glo™ CYP3A4 Screening Systems (Promega) according to the instructions provided by the manufacturer.

4.4. In vivo evaluation

4.4.1. Animals. Female CD-1 and athymic nude *nu/nu* CD-1 mice (6–8 weeks, 25–29 g) were obtained from Charles River Laboratories (Wilmington, MA). Animals were allowed to acclimate for a minimum of one week prior to initiation of a study. Female Sprague–Dawley rats with implanted jugular vein canulas were obtained from Hilltop Lab Animals (Scottsdale, PA) and were allowed to acclimate for a minimum of 1 day prior to a study. Throughout the studies, animals were allowed sterile rodent chow and water ad libitum, and immunocompromised animals were maintained under specific pathogen-free conditions. All rodent animal studies were conducted at OSI facilities with the approval of the Institutional Animal Care and Use Committee in an American Association for Accreditation of Laboratory Animal Care (AAALAC)-accredited vivarium and in accordance with the Institute of Laboratory Animal Research (Guide for the Care and Use of Laboratory Animals, NIH, Bethesda, MD). Animals for pharmacokinetic studies on male Beagle dogs were housed at MPI Research (Mattawan, MI).

4.4.2. Pharmacokinetic analysis of AQIP. For pharmacokinetic analysis, the compound was formulated in saline adjusted to pH 2 with 0.01 mol/L hydrochloric acid for intravenous injection and in 25 mmol/L tartaric acid for oral administration. Female CD-1 mice (6–8 weeks old) received either a single intravenous dose (5 mg/kg) or a single oral dose (25 mg/kg) of compound. For intravenous dosing, compound was delivered via tail vein injection at a dosing volume of 4 mL/kg. For oral dos-

ing, compound was delivered via oral gavage in a dosing volume of 10 mL/kg. Subsequently, three animals were sacrificed at each designated timepoint and blood samples were collected in EDTA. After centrifugation at 1500g for 10 min, plasma samples were prepared by protein precipitation with methanol and analyzed by HPLC–MS/MS (PE Sciex API 3000 LC/MS/MS System, Applied Biosystems). Pharmacokinetic parameters for the plasma time-concentration profile, including C_{max} , AUC, elimination half-life ($t_{1/2}$), volume of distribution at steady state (V_{ss}), clearance (Cl), and oral bioavailability, were calculated by non-compartmental analysis.

4.4.3. In vivo antitumor efficacy study. Cells were harvested from cell culture flasks during exponential cell growth, washed twice with sterile PBS, counted, and resuspended in PBS to a suitable concentration before sc implantation on the right flank of *nu/nu* CD-1 mice. Tumors were established to $200 \pm 50 \text{ mm}^3$ in size before randomization into treatment groups of 8 mice each for efficacy studies. Designated compound or vehicle was administered orally as indicated. Body weights were determined twice weekly along with tumor volume $\{V = [\text{length} \times (\text{width})^2]/2\}$ measurements using Vernier calipers during the study. Tumor growth inhibition (TGI) was determined by the following formula: $\%TGI = (1 - \{(T_t/T_0)/(C_t/C_0)\} / 1 - \{C_0/C_1\}) \times 100$ where the median tumor volumes of treated (T) and control (C) animals were determined at both time 0 and time t . The %TGI values indicated are the mean %TGI over the entire dosing period. Tumor growth inhibition of $\geq 50\%$ is considered significant. Growth delay is calculated as $T - C$ where T and C are the times in days for mean tumor size in the treated (T) and control (C) groups to reach 400% of the initial tumor volume.

4.4.4. Glucose tolerance test. Tests were performed as described in Haluzik et al., *Diabetes* **2003**, *52*, 2483–2489. Briefly, CD-1 mice were dosed orally for 3 consecutive days with AQIP or vehicle. Mice were fasted for 8 h (water ad libitum) prior to final administration of treatments. Glucose (D-dextrose in water for injection, 20% solution) was administered at 2 g/kg by intraperitoneal injection immediately following the 3rd oral dose of compound. Blood samples were collected for glucose evaluation by tail vein stick at various time points following final compound dosing. Blood glucose levels were measured using a Glucose-201 instrument from HemoCue, Inc. Plasma insulin levels at 4 h post the last dose were determined using a rat/mouse insulin ELISA kit (Linco Research, Inc.).

Acknowledgments

We thank Drs. Jonathan Pachter and Lee Arnold for consultation and critical review; Ms. Viorica M. Lazarescu and Dr. Minghui Wang for analytical support; and Mr. Paul Maresca, Ms. Jo Dunseath, Mr. Pete Meyn, and the Leads Discovery Group for conducting in vitro ADMET studies.

References and notes

- LeRoith, D.; Werner, H.; Neuenschwander, S.; Kalebic, T.; Helman, L. J. *Ann. NY Acad. Sci.* **1995**, *766*, 402–408.
- Larsson, O.; Girnita, A.; Girnita, L. *Br. J. Cancer* **2005**, *92*, 2097–2101.
- Furukawa, M.; Raffeld, M.; Mateo, C.; Sakamoto, A.; Moody, T. W.; Ito, T.; Venzon, D. J.; Serrano, J.; Jensen, R. T. *Clin. Cancer Res.* **2005**, *11*, 3233–3242.
- Pollak, M. N.; Schernhammer, E. S.; Hankinson, S. E. *Nat. Rev. Cancer* **2004**, *4*, 505–518.
- Grimberg, A.; Cohen, P. J. *Cell Physiol.* **2000**, *183*, 1–9.
- Adams, T. E.; Epa, V. C.; Garrett, T. P. J.; Ward, C. W. *Cell. Mol. Life Sci.* **2000**, *57*, 1050–1093.
- LeRoith, D.; Roberts, C. T., Jr. *Cancer Lett.* **2003**, *195*, 127–137.
- Baserga, R.; Peruzzi, F.; Reiss, K. *Int. J. Cancer* **2003**, *107*, 873–877.
- Butler, A. A.; Yakar, S.; Gewolb, I. H.; Karas, M.; Okubo, Y.; LeRoith, D. *Comp. Biochem. Physiol. B* **1998**, *121*, 19–26.
- Quinn, K. A.; Treston, A. M.; Unsworth, E. J.; Miller, M.-J.; Vos, M.; Grimley, C.; Battey, J.; Mulshine, J. L.; Cuttitta, F. J. *Biol. Chem.* **1996**, *271*, 11477–11483.
- Ma, J.; Pollak, M. N.; Giovannucci, E.; Chan, J. M.; Tao, Y.; Hennekens, C. H.; Stampfer, M. J. *J. Natl. Cancer Inst.* **1999**, *91*, 620–625.
- Chan, J. M.; Stampfer, M. J.; Giovannucci, E.; Gann, P. H.; Ma, J.; Wilkinson, P.; Hennekens, C. H.; Pollak, M. *Science* **1998**, *279*, 563–566.
- Hankinson, S. E.; Willett, W. C.; Colditz, G. A.; Hunter, D. J.; Michaud, D. S.; Deroo, B.; Rosner, B.; Speizer, F. E.; Pollak, M. *Lancet* **1998**, *351*, 1393–1396.
- Yu, H.; Spitz, M. R.; Mistry, J.; Gu, J.; Hong, W. K.; Wu, X. *J. Natl. Cancer Inst.* **1999**, *91*, 151–156.
- Zhao, H.; Grossman, H. B.; Spitz, M. R.; Lerner, S. P.; Zhang, K.; Wu, X. *J. Urol.* **2003**, *169*, 714–717.
- Parker, A. S.; Cheville, J. C.; Janney, C. A.; Cerhan, J. R. *Hum. Pathol.* **2002**, *33*, 801–805.
- Zhang, L.; Zhou, W.; Velculescu, V. E.; Kern, S. E.; Hruban, R. H.; Hamilton, S. R.; Vogelstein, B.; Kinzler, K. W. *Science* **1997**, *276*, 1268–1272.
- Hassan, A. B.; Macaulay, V. M. *Ann. Oncol.* **2002**, *13*, 349–356.
- Chen, C.-L.; Ip, S.-M.; Cheng, D.; Wong, L.-C.; Ngan, H. Y. S. *Clin. Cancer Res.* **2000**, *6*, 474–479.
- Kalli, K. R.; Falowo, O. I.; Bale, L. K.; Zschunke, M. A.; Roche, P. C.; Conover, C. A. *Endocrinology* **2002**, *143*, 3259–3267.
- Kondo, M.; Suzuki, H.; Ueda, R.; Osada, H.; Takagi, K.; Takahashi, T.; Takahashi, T. *Oncogene* **1995**, *10*, 1193–1198.
- Wang, Z.; Ruan, Y. B.; Guan, Y.; Liu, S. H. *World J. Gastroenterol.* **2003**, *9*, 267–270.
- Cui, H.; Cruz-Correa, M.; Giardiello, F. M.; Hutcheon, D. F.; Kafonek, D. R.; Brandenburg, S.; Wu, Y.; He, X.; Powe, N. R.; Feinberg, A. P. *Science* **2003**, *299*, 1753–1755.
- (a) Min, Y.; Adachi, Y.; Yamamoto, H.; Ito, H.; Itoh, F.; Lee, C.-T.; Nadaf, S.; Carbone, D. P.; Imai, K. *Cancer Res.* **2003**, *63*, 6432–6441; (b) Jernberg-Wiklund, H.; Nilsson, K. *Adv. Cancer Res.* **2007**, *97*, 139–165.
- Resnicoff, M.; Coppola, D.; Sell, C.; Rubin, R.; Ferrone, S.; Baserga, R. *Cancer Res.* **1994**, *54*, 4848–4850.
- Chernicky, C. L.; Yi, L.; Tan, H.; Gan, S. U.; Ilan, J. *Cancer Gene Ther.* **2000**, *7*, 384–395.
- Maloney, E. K.; McLaughlin, J. L.; Dagdigian, N. E.; Garrett, L. M.; Connors, K. M.; Zhou, X.-M.; Blättler,

- W. A.; Chittenden, T.; Singh, R. *Cancer Res.* **2003**, *63*, 5073–5083.
28. Wang, Y.; Hailey, J.; Williams, D.; Wang, Y.; Lipari, P.; Malkowski, M.; Wang, X.; Xie, L.; Li, G.; Saha, D.; Ling, W. L. W.; Cannon-Carlson, S.; Greenberg, R.; Ramos, R. A.; Shields, R.; Presta, L.; Brams, P.; Bishop, W. R.; Pachter, J. A. *Mol. Cancer Ther.* **2005**, *4*, 1214–1221.
29. Cohen, B. D.; Baker, D. A.; Soderstrom, C.; Tkalcevic, G.; Rossi, A. M.; Miller, P. E.; Tengowski, M. W.; Wang, F.; Gualberto, A.; Beebe, J. S.; Moyer, J. D. *Clin. Cancer Res.* **2005**, *11*, 2063–2073.
30. Goetsch, L.; Gonzalez, A.; Leger, O.; Beck, A.; Pauwels, P. J.; Haeuw, J. F.; Corvaia, N. *Int. J. Cancer* **2005**, *113*, 316–328.
31. Prager, D.; Li, H.-L.; Asa, S.; Melmed, S. *Proc. Natl. Acad. Sci. U.S.A.* **1994**, *91*, 2181–2185.
32. Kalebic, T.; Blakesley, V.; Slade, C.; Plasschaert, S.; LeRoith, D.; Helman, L. J. *Int. J. Cancer* **1998**, *76*, 223–227.
33. Scotlandi, K.; Avnet, S.; Benini, S.; Manara, M. C.; Serra, M.; Cerisano, V.; Perdichizzi, S.; Lollini, P.-L.; De Giovanni, C.; Landuzzi, L.; Picci, P. *Int. J. Cancer* **2002**, *101*, 11–16.
34. (a) García-Echeverría, C.; Pearson, M. A.; Marti, A.; Meyer, T.; Mestan, J.; Zimmermann, J.; Gao, J.; Bruegen, J.; Capraro, H.-G.; Cozens, R.; Evans, D. B.; Fabbro, D.; Furet, P.; Porta, D. G.; Liebetanz, J.; Martiny-Baron, G.; Ruetz, S.; Hofmann, F. *Cancer Cell* **2004**, *5*, 231–239; (b) Warshamana-Greene, G. S.; Litz, J.; Buchdunger, E.; García-Echeverría, C.; Hofmann, F.; Krystal, G. W. *Clin. Cancer Res.* **2005**, *11*, 1563–1571.
35. (a) Haluska, P.; Carboni, J. M.; Loegering, D. A.; Lee, F. Y.; Wittman, M.; Saulnier, M. G.; Frennesson, D. B.; Kalli, K. R.; Conover, C. A.; Attar, R. M.; Kaufmann, S. H.; Gottardis, M.; Erlichman, C. *Cancer Res.* **2006**, *66*, 362–371; (b) Velaparthi, U.; Wittman, M.; Liu, P.; Stoffan, K.; Zimmermann, K.; Sang, X.; Carboni, J.; Li, A.; Attar, R.; Gottardis, M.; Greer, A.; Chang, C. Y.; Jacobsen, B. L.; Sack, J. S.; Sun, Y.; Langley, D. R.; Balasubramanian, B.; Vyas, D. *Bioorg. Med. Chem. Lett.* **2007**, *17*, 2317–2321.
36. Mulvihill, M. J.; Ji, Q.-S.; Werner, D.; Beck, P.; Cesario, C.; Cooke, A.; Cox, M.; Crew, A.; Dong, H.; Foreman, K. W.; Mak, G.; Nigro, A.; O'Connor, M.; Saroglou, L.; Stolz, K. M.; Sujka, I.; Volk, B.; Weng, Q.; Wilkes, R. *Bioorg. Med. Chem. Lett.* **2007**, *17*, 1091–1097.
37. García-Echeverría, C. *IDrugs* **2006**, *9*, 415–419.
38. Surmacz, E. *Oncogene* **2003**, *22*, 6589–6597.
39. Foreman, K. W.; Mulvihill, M. J.; Ji, Q.-S.; Hubbard, S.; Miller, T. *Protein: Structure, Function and Bioinformatics*, to be submitted for publication.
40. Gilman, H.; Christian, R. V.; Spatz, S. M. *J. Am. Chem. Soc.* **1946**, *68*, 979–981.
41. Plobeck, N.; Delorme, D.; Wei, Z.-Y.; Yang, H.; Zhou, F.; Schwarz, P.; Gawell, L.; Gagnon, H.; Pelcman, B.; Schmidt, R.; Yue, S. Y.; Walpole, C.; Brown, W.; Zhou, E.; Labarre, M.; Payza, K.; St-Onge, S.; Kamassah, A.; Morin, P.-E.; Projean, D.; Ducharme, J.; Roberts, E. *J. Med. Chem.* **2000**, *43*, 3878–3894.
42. Turck, A.; Mojovic, L.; Quéguiner, G. *Synthesis* **1988**, *11*, 881–884.
43. (a) Abushanab, E.; Bindra, A. P.; Goodman, L. *J. Heterocycl. Chem.* **1975**, *12*, 207–209; (b) Hartz, R. A.; Gilligan, P. J.; Nanda, K. K.; Tebben, A. J.; Fitzgerald, L. W.; Miller, K. *Bioorg. Med. Chem. Lett.* **2002**, *12*, 291–294.
44. Arnold, L. D.; Cesario, C.; Coate, H.; Crew, A. P.; Dong, H.; Foreman, K.; Honda, A.; Laufer, R.; Li, A. H.; Mulvihill, K. M.; Mulvihill, M. J.; Nigro, A.; Panicker, B.; Steinig, A. G.; Sun, Y.; Weng, Q.; Werner, D. S.; Wyle, M. J.; Zhang, T. WO 2005097800 A1.
45. Kabalka, G. W.; Shoup, T. M.; Goudgaon, N. M. *J. Org. Chem.* **1989**, *54*, 5930–5933.
46. Favelyukis, S.; Till, J. H.; Hubbard, S. R.; Miller, W. T. *Nat. Struct. Biol.* **2001**, *8*, 1058–1063.
47. Ji, Q.-S.; Winnier, G. E.; Niswender, K. D.; Horstman, D.; Wisdom, R.; Magnuson, M. A.; Carpenter, G. *Proc. Natl. Acad. Sci. U.S.A.* **1997**, *94*, 2999–3003.